

Review

A Comprehensive Review of Methods for Hydrological Forecasting Based on Deep Learning

Xinfeng Zhao ¹, Hongyan Wang ², Mingyu Bai ², Yingjie Xu ², Shengwen Dong ^{3,*}, Hui Rao ⁴ and Wuyi Ming ^{2,5,*}

¹ College of Water Conservancy Engineering, Yellow River Conservancy Technical Institute, Kaifeng 475000, China; zhaoxinfeng@yrcti.edu.cn

² Henan Key Laboratory of Intelligent Manufacturing of Mechanical Equipment, Zhengzhou University of Light Industry, Zhengzhou 450002, China; hongyanwang923@163.com (H.W.); wl1291242215@163.com (M.B.); xyj15203873137@163.com (Y.X.)

³ Hubei Water Resources and Hydropower Science and Technology Promotion, Hubei Water Resources Research Institute, Wuhan 430070, China

⁴ Technical Research and Development Department, Wuhan Jianglai Measuring Equipment Co., Ltd., Wuhan 430074, China; hui.rao@163.com

⁵ Guangdong Provincial Key Laboratory of Digital Manufacturing Equipment, Guangdong HUST Industrial Technology Research Institute, Dongguan 523808, China

* Correspondence: sky310@foxmail.com (S.D.); mingwuyi@gmail.com (W.M.)

Abstract: Artificial intelligence has undergone rapid development in the last thirty years and has been widely used in the fields of materials, new energy, medicine, and engineering. Similarly, a growing area of research is the use of deep learning (DL) methods in connection with hydrological time series to better comprehend and expose the changing rules in these time series. Consequently, we provide a review of the latest advancements in employing DL techniques for hydrological forecasting. First, we examine the application of convolutional neural networks (CNNs) and recurrent neural networks (RNNs) in hydrological forecasting, along with a comparison between them. Second, a comparison is made between the basic and enhanced long short-term memory (LSTM) methods for hydrological forecasting, analyzing their improvements, prediction accuracies, and computational costs. Third, the performance of GRUs, along with other models including generative adversarial networks (GANs), residual networks (ResNets), and graph neural networks (GNNs), is estimated for hydrological forecasting. Finally, this paper discusses the benefits and challenges associated with hydrological forecasting using DL techniques, including CNN, RNN, LSTM, GAN, ResNet, and GNN models. Additionally, it outlines the key issues that need to be addressed in the future.

Keywords: hydrological forecasting; deep learning; data-driven; prediction; critical review



Citation: Zhao, X.; Wang, H.; Bai, M.; Xu, Y.; Dong, S.; Rao, H.; Ming, W. A Comprehensive Review of Methods for Hydrological Forecasting Based on Deep Learning. *Water* **2024**, *16*, 1407. <https://doi.org/10.3390/w16101407>

Academic Editor: Fi-John Chang

Received: 12 April 2024

Revised: 7 May 2024

Accepted: 13 May 2024

Published: 15 May 2024



Copyright: © 2024 by the authors. Licensee MDPI, Basel, Switzerland. This article is an open access article distributed under the terms and conditions of the Creative Commons Attribution (CC BY) license (<https://creativecommons.org/licenses/by/4.0/>).

1. Introduction

In 2021, the journal *Nature* showcased a recent study on global flood hazard analysis online in the form of a cover article. The findings indicate a consistent annual increase in the proportion of the global population that is vulnerable to flooding [1]. Floods stand as one of the most prevalent natural disasters globally. With an escalation in both the frequency and intensity of heavy rainfall, coupled with a recurring pattern, catastrophic flood events are being witnessed across various regions worldwide, significantly impacting human productivity and livelihoods [2,3]. Generally speaking, river and coastal system flooding represents the most prevalent and devastating climate-related disaster, inflicting billions of dollars in damages annually. These impacts disproportionately affect impoverished and vulnerable communities, as floods severely disrupt their livelihoods and they possess a limited capacity to rebound from such disasters [4–6]. For instance, Henan, China experienced an abnormally strong downpour in July 2021 that peaked at 646 mm in a 24 h period, which is equal to the region's average yearly precipitation. This resulted in direct economic damage amounting to USD 17.8 billion [7]. In September 2023, the Mediterranean

hurricane Storm Daniel caused a landfall on the eastern Mediterranean coast of Libya and caused flooding that collapsed the Abu Mansour and Bilad reservoir dams upstream of the city of Derna. This catastrophe devastated approximately 25% of the city due to the massive currents of water and mud, resulting in the loss of over 4000 lives and leaving around 10,000 individuals unaccounted for [8]. Human beings have proven through years of struggling with floods that combining engineering and non-engineering measures is an effective measure for solving the problem of floods [9–11]. In addition, among the usual non-engineering measures, continuous efforts are made to enhance the precision of hydrological forecasting, a strategy that has proven to be effective.

Hydrological forecasting is the use of hydrological change patterns to analyze and calculate the hydrological elements of the studied area to reveal and predict future changes in these hydrological elements for an applied discipline. For instance, hydrological forecasting may utilize past or present hydrometeorological data, encompassing a basin, region, or specific hydrological station, to make qualitative or quantitative predictions regarding future hydrological conditions. Such forecasts hold critical significance for flood control, drought management, water resource allocation, and national defense strategies. To enhance the accuracy and reliability of hydrological forecasting, researchers have proposed numerous methods from various angles, integrating insights from related disciplines [12]. These methods can be broadly classified into two categories: traditional methods and new methods. The former mainly include cause analyses and hydrological statistical methods, and the latter mainly include artificial neural networks, grey system analyses, fuzzy mathematical models, and other methods.

Artificial intelligence (AI) has experienced rapid development over the past three decades, finding widespread application across various disciplines and yielding significant results. Especially in the context of the development of big data, AI has set off a new wave of the digital revolution. Deep learning (DL) is a new research direction in the field of machine learning (ML), which has been introduced into ML to bring it closer to its original goal, AI. Building models with higher processing capacities and prediction accuracy, which minimizes the need for human intervention and experience, and serving as an exploratory data-mining tool to facilitate discovery that expands current knowledge and capabilities are two of DL's primary purposes [13]. In 2016, AlphaGo's victory over Lee Sedol, a nine-dan professional chess player, with a decisive 4:1 margin exemplified AI's prowess, subsequently propelling it into the limelight of research as a prominent keyword [14]. In 2022, AlphaFold2 utilized protein structure prediction models through "end-to-end" neural networks for predicting protein structures in three dimensions. These trained neural networks have the capability to predict protein properties from gene sequences, and AlphaFold2 has already predicted 98.5% of the structures of human proteins, a significant advancement compared to the previous coverage of only 17% of amino acid residues in human protein sequences after decades of scientific effort [15]. In addition, DL, renowned for its adeptness in discerning intricate data patterns and autonomously extracting features, has found extensive application in materials science [16,17], new energy [18–20], medicine [21–23], and engineering [24–26]. The success of these applications has spurred the further expansion of the DL approach into diverse domains. For solving the time-series prediction problem, the DL analysis method has also been applied in the fields of electric power [27,28], meteorology [29–31], and finance [32,33] through continuous improvement, achieving good results in long- and short-term prediction.

Recently, DL has emerged as a transformative and multifaceted tool, revolutionizing industrial applications and enhancing capabilities for scientific discovery and model development. The use of DL techniques in flood management has been on the rise, aimed at addressing the challenges posed by precise yet time-consuming numerical modeling [34,35]. Enhancing and refining hydrological time-series prediction technology through the integration of the DL approach to comprehend and elucidate the evolving patterns of hydrological time series has emerged as a focal area of research. Therefore, we provide a comprehensive overview of the latest advancements in applying DL methods to hydrological forecast-

ing. This study diverges from previous reviews primarily in its assessment of prediction challenges outlined in the literature, the elaboration on algorithmic enhancements, a side-by-side comparison of prediction accuracies and computational costs, and an analysis of their practical utility in engineering applications. The rest of the review paper is organized as follows: Section 2 reviews the application of convolutional neural networks (CNNs) and recurrent neural networks (RNNs) in hydrological forecasting and compares their performance in terms of improvements, prediction accuracy, and computational costs. In Section 3, we demonstrate the application of long short-term memory (LSTM) in hydrological forecasting, especially basic LSTM and improved LSTM, and analyze the application effects and development trends of these models. In Section 4 we estimate the performance of GRUs and other models, such as generative adversarial networks (GANs), residual networks (ResNets), and graph neural networks (GNNs), for hydrological forecasting. In Section 5, we discuss the trend of DL algorithms, such as CNNs, RNNs, LSTM, GRUs, and others, in hydrological prediction, with a particular focus on discerning differences among these algorithms. Section 6 gives a summary of the full text and looks forward to the key problems that need to be solved in future research.

2. CNNs/RNNs for Hydrological Forecasting

2.1. Principle of CNNs/RNNs

In DL, CNNs are a class of artificial neural networks (ANNs), which belong to feedforward neural networks [36]. Moreover, CNNs stand out as prominent algorithms within the domain of DL [37], recognized for their shift-invariant or spatially invariant nature. A CNN usually consists of the following layers: the convolutional layer (Convolution Operation), the pooling layer (Subsampling Operation), and the fully connected layer (SoftMax Operation), as shown in Figure 1a. The CNN model was proposed by Yann Lecun of New York University in 1998 (LeNet-5), and fundamentally operates as a multi-layer perceptual machine. The success of CNNs can be attributed to their utilization of local connectivity and weight sharing. This approach not only decreases the number of weights, simplifying network optimization, but also reduces the model's complexity and the likelihood of overfitting.

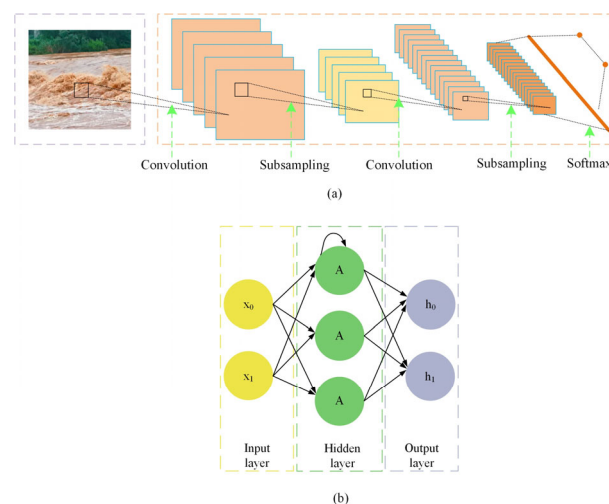


Figure 1. Structural diagrams of a CNN and an RNN: (a) CNN; (b) RNN.

RNNs are a class of recurrent neural networks designed to process sequence data. In an RNN, information cycles through the network in a sequential manner, with each node (referred to as a recurrent unit) connected in a chain. This architecture is grounded in the notion that “human cognition relies on past experiences and memories”. The basic layers of an RNN include input, hidden, and output layers, as shown in Figure 1b. Due to their recursive structure, RNNs are adept at addressing sequence modeling challenges and find

utility across diverse domains, including text generation, machine translation, and image captioning [38,39].

2.2. CNNs for Prediction

Sepahvand et al. [40] compared the performance of a learning-based CNN algorithm with support vector regression (SVR) and group method of data handling (GMDH)-based algorithms for hydrological infiltration modeling. The study area consisted of cumulative infiltration data from 16 stations in the provinces of Illam and Lorestan in western Iran, which were collected using a double-ring penetrometer. Their experimental findings demonstrated the superior performance of the CNN model ($R^2 = 0.97$, Nash efficiency coefficient (NSE) = 0.97) compared to SVR ($R^2 = 0.87$, NSE = 0.806) and GMDH ($R^2 = 0.92$, NSE = 0.915). This research aimed to provide valuable insights for urban flood management and warning systems. Han et al. [41] proposed an experimental automatic urban road inundation monitoring method based on the YOLOv2 framework (in Figure 2). Their experimental results showed that the validation of the model had a high average accuracy of 90.1% for flood detection, while its average training accuracy was 96.1%. Although their model is more accurate, it requires a large training dataset. Additionally, it lacks the capability to forecast future hydrological phenomena, such as alterations in flood duration and coverage. For flood prediction, most of the algorithms used are based on CNNs. Nonetheless, alternative architectures, such as hybrid CNN-LSTM algorithms, have demonstrated potential in elevating the precision of flood prediction outcomes [42]. Windheuser et al. [43] proposed a fully automated end-to-end image detection system using the fusion of multiple deep neural networks, including the CNN and LSTM models, to predict flood levels from two USGS gauging stations, Columbus River and Sweetwater River, Georgia, USA. Their experimental results demonstrated that the proposed model predicted NSEs of historical water gauge height data of 85% for 6 h, 96% for 12 h, 96% for 24 h, and 95% for 48 h at Columbus station, and that the short-term NSEs were greater than 83% at Sweetwater Creek Station. These findings underscore the potential of employing a hybrid end-to-end DL model, leveraging extensive image data, for practical engineering applications in short- and medium-term flood forecasting at regional scales. Sharma and Kumari [44] combined a CNN with the random forest (RF) and SVR techniques to construct CNN-RF and CNN-SVR hybrid models for flood forecasting, which were compared with RF, SVR, and ANN methods. Their experimental results demonstrated that the performance of the CNN-RF model exceeded that of the other models at both the Kantamal and Kesinga hydrological stations. At the Kantamal hydrological station, the R^2 values of the CNN-RF and CNN-SVR models were 0.95 and 0.92, respectively. The CNN approach can be considered a valuable technique for feature extraction in flood forecasting, with the potential to enhance the overall predictive accuracy. Li et al. [45] proposed a rainfall-runoff model based on CNN-LSTM, which directly calculates watershed runoff from two-dimensional radar images of rainfall. The study area chosen was the Elbe River basin in Saxony, Germany. It was found that during low- and high-water-level periods, the NSE fluctuated between 0.63 and 0.86, and between 0.46 and 0.97, respectively. This indicates that CNN-LSTM contributes to estimating water resource availability and flood alerts for watershed management. Aderyani et al. [46] compared the performance of three machine learning and DL-based rainfall forecasting methods, namely SVR, LSTM, and a CNN (in Figure 3), using a dataset from the Niavaran station in Tehran, Iran. Their experimental results showed that the CNN model was slightly weaker than the other two models in over-forecasting 5 min and 15 min rainfall, and the R^2 values of the CNN model for these two durations of rainfall were 0.672 and 0.491, respectively. This implies that the prediction performance of the CNN model is still worse than that of the optimized traditional machine learning model. However, it is feasible to use the CNN model for short-term hydrological forecasting, and achieving better performance may require further optimization of the model. The scarcity of high-resolution urban digital elevation model (DEM) datasets, particularly in some developing countries, poses challenges for flood risk

management. Jiang et al. [47] proposed a multi-scale mapping framework based on a CNN (MSM-CNN), which may contribute to addressing the data scarcity issues in urban flood modeling and hydraulic engineering applications. Their results confirmed that MSM-CNN effectively restored high-resolution urban DEMs from 2, 4, and 8 m to 0.5 m. This means that the MSM-CNN model could provide a cost-effective innovative approach for obtaining high-resolution DEMs in data-scarce regions.

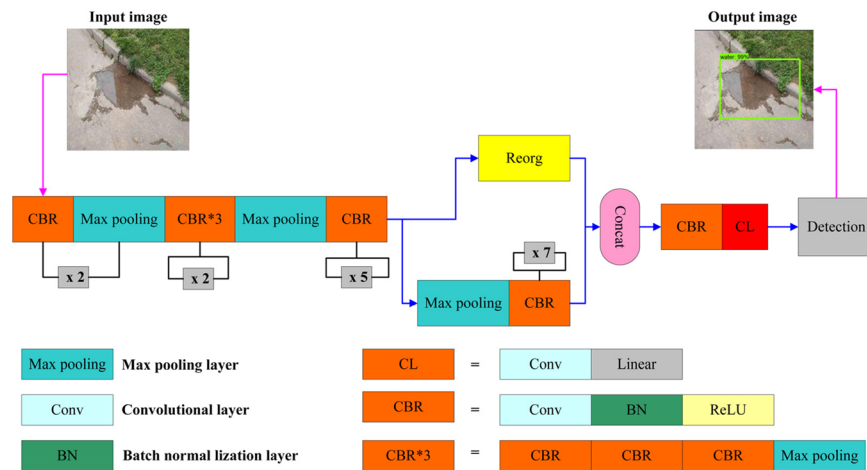


Figure 2. Flowchart of the urban road flood detection method based on YOLOv2 [41].

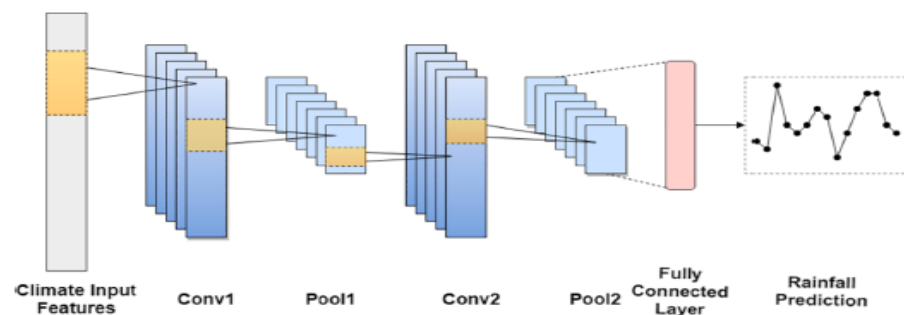


Figure 3. Architecture of a one-dimensional CNN for rainfall prediction in hydrological forecasting [48].

2.3. RNNs for Prediction

For the complex problem of predicting time-varying water resources, Coulibaly et al. [49] proposed a dynamic RNN method that automatically selects the optimally trained network to predict different non-stationary hydrological time series. Performance comparisons based on hydrological time-series data from three selected sites, namely the Saint Lawrence River (SLR) in Cornwall, the Great Salt Lake (GSL), and the Nile River, are shown in Figure 4. It was found that the dynamically driven RNN model with Bayesian regularization (RNN-BR) outperformed the traditional multivariate adaptive regression spline (MARS) model, which is ideal for modeling the complex dynamics of hydrological systems. Nonlinear prediction of non-stationary time series is a difficult task [50], and this study shows a pioneering use of the RNN approach for the hydrological prediction of non-stationary states and achieved more obvious positive results. Güldal and Tongal [51] constructed RNN models with different input structures and compared them with adaptive network-based fuzzy inference systems and autoregressive moving-average models for lake water level prediction. Conducted in the western region of the Turkish Taurus Mountains, the study revealed that the R^2 values of the RNN models ranged from 0.95 to 0.99, surpassing the R^2 values of 0.78 to 0.93 for the adaptive network-based fuzzy inference system models and autoregressive models. This indicates the suitability of RNN models

for predicting lake water level changes, offering higher accuracy and reliability. Cai and Yu [52] proposed a hybrid recurrent neural network (HRNN) that combines RNN and autoregressive integrated moving-average model methods for forecasting flood trends and peak times during flood seasons. The model was tested using four flood events from 2019 as a validation dataset, revealing an NSE of 0.937 for the HRNN model, surpassing both the Bi-LSTM model (NSE of 0.833) and the Xin'anjiang model (NSE of 0.831). These results indicate the efficiency of the HRNN model in predicting flood inflows compared to traditional hydrological models and other machine learning networks. Kim et al. [53] investigated the optimal DL models for inflow prediction at Andong Dam and Imhae Dam, located in the upper Nakdong River in South Korea. Using nearly 20 years of hydrological data, their experimental results showed that the RNN for Andong Dam and the LSTM for Imhae Dam served as the optimal models for each dam during the drought period with the smallest percent differences between observations, at 4% and 2%, respectively. Under typhoon conditions, the Gate Recurrent Unit at Andong Dam and the RNN at Imhae Dam were selected as the best models, with the GRU and RNN results differing from the observed maximum inflow by 2% and 6%, respectively (typhoon "Memi" scenario). This investigation underscores the importance of comparing the accuracy of DL models in inflow prediction for making informed decisions in the efficient operation and management of dams. Wang et al. [54] constructed LSTM and RNN models, analyzing the structural disparities and impacts on processing flood data between the two models and comparing their performance in flood forecasting. Their results indicated that within a 1 h forecasting period at Loudi Station, the NSE of the RNN model with an identical structure and hyperparameters was 0.9789, surpassing that of the LSTM model at 0.9621. The simpler internal structure of the RNN model renders it more suitable for flood forecasting tasks. Karbasi et al. [55] proposed a hybrid technique using time-varying filter-based empirical modal decomposition (TVF-EMD) and DL to predict weekly reference evapotranspiration and compared four machine learning methods, namely the bidirectional recurrent neural network (BiRNN), multi-layer perceptual neural network (MLP), RF, and extreme gradient-boosting (XGBoost) methods, in terms of their prediction performance. Their results demonstrated that the TVF-BiRNN model achieved the highest accuracy in simulating weekly reference evapotranspiration at the Redcliffe and Gold Coast stations (Redcliffe: $R = 0.93$, $MAPE = 9.20\%$, $RMSE = 3.88$ mm/week; Gold Coast: $R = 0.87$, $MAPE = 11.54\%$, $RMSE = 4.12$ mm/week). This indicates that by enhancing the structure of an RNN, its predictive accuracy for hydrological forecasting surpasses that of traditional machine learning methods such as MLP, RFs, and XGBoost. For dam inflow prediction, Ayele et al. [56] compared the performance of RNN, BiRNN, and GRU prediction models and made a prediction that the Kesem Dam could be overtopped by a flood with a return period of approximately 10,000 years to determine if the existing structure provides an adequate level of safety. This illustrates that enhancing the structure of the RNN can enhance the prediction accuracy of the model for medium- and long-term datasets, facilitating its practical application in engineering projects.

Moreover, certain studies have successfully integrated spatial distribution with RNNs, leading to enhanced accuracy in hydrological forecasting, especially for geospatial forecasting. Wang et al. [57] proposed a new model named RNN-RandExtreme, coupling an RNN with random generation methods, to improve the accuracy of predicting downscaling extreme precipitation. Their experimental findings indicated that leveraging extensive datasets from various regions of China resulted in a notable improvement in the prediction accuracy of RNN-RandExtreme for extreme precipitation, with enhancements of 28.32% and 16.56%, respectively, compared to both an ANN and a standalone RNN model. The accuracy of hydrological forecasts is directly affected by the statistical downscaling of time-series features; this is due to the fact that meteorological data have distinct time-series features, and the use of finer-grained data facilitates the improvement of forecast accuracy. Kao et al. [58] introduced a novel machine learning-based model integrating a stacked autoencoder (SAE) with an RNN, referred to as SAE-RNN. They utilized an

extensive dataset detailing hour-by-hour flood inundation depths for the model's training, validation, and testing stages. The findings indicated that the RMSE values were notably low (<0.09 m) and the R^2 values were significantly high (>0.95) across all three phases for 1–3 h predictions. The model's successful prediction capabilities are attributed to its efficient sequential extraction of nonlinear dependence structures from flood dynamics. This efficiency in reducing hydrological uncertainty is achieved through the use of the SAE, coupled with the transformation of rainfall sequences into future flood features via the RNN. Huang [59] devised a novel method to predict the flooding of coastal areas effectively by integrating detailed analyses of various hydrological and geomorphological factors into an RNN model, as depicted in Figure 5. The experimental results indicated that the flood prediction maps of the proposed RNN model were comparable to the flood maps generated using the traditional numerical hydrological model, but the computational speed of the RNN model could be at least 322 times faster than the numerical inundation model. In addition, the training procedure for the RNN could significantly reduce the mean relative error (MRE) value from an average of 0.338 to 0.055 compared to the traditional numerical training procedure. In Huang's study, an innovative RNN model is used to establish coupling relationships between geomorphological factors, such as the local upslope areas contributing to floods, flow path lengths along the coastline, and flood depths at any location in the watershed, so as to efficiently and accurately characterize the spatial and temporal behaviors of floods at the surface.

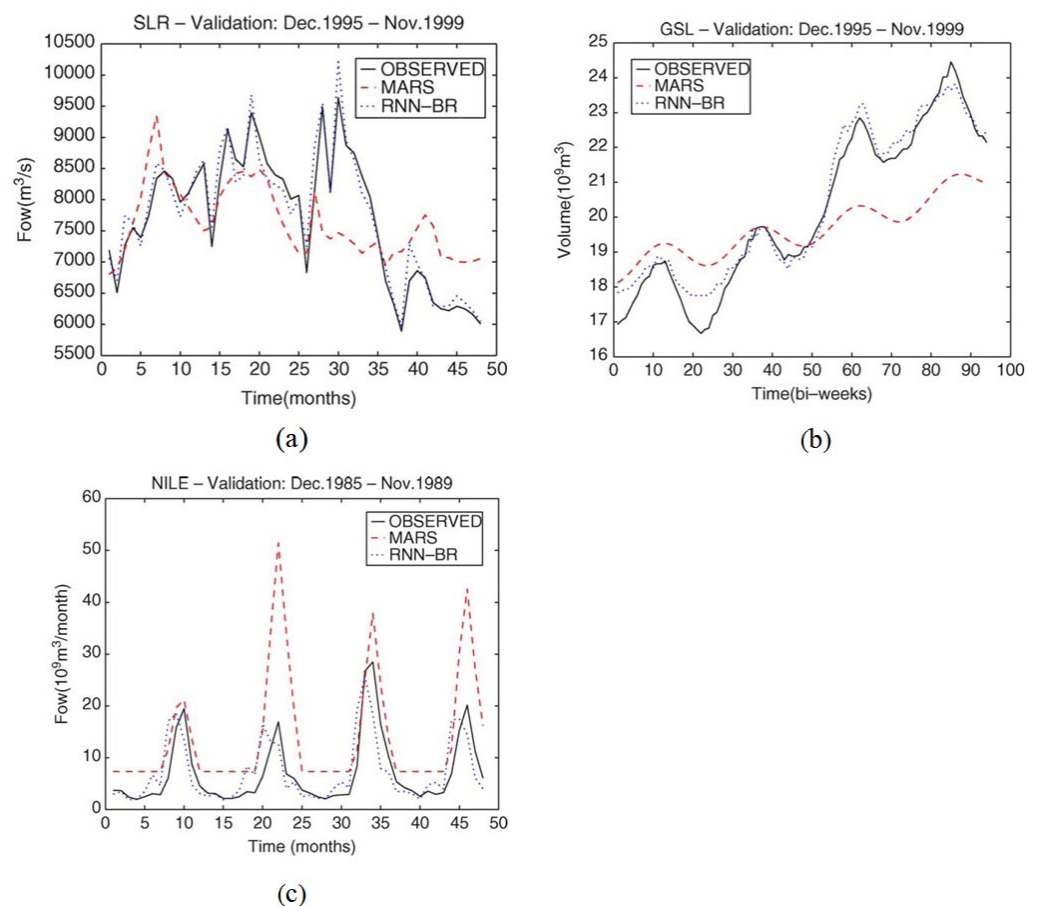


Figure 4. Observed and predicted hydrological time series at three selected locations: (a) SLR's monthly flow; (range: 5500–10,500) (b) GSL's bi-weekly volume; (c) Nile River's monthly flow [49].

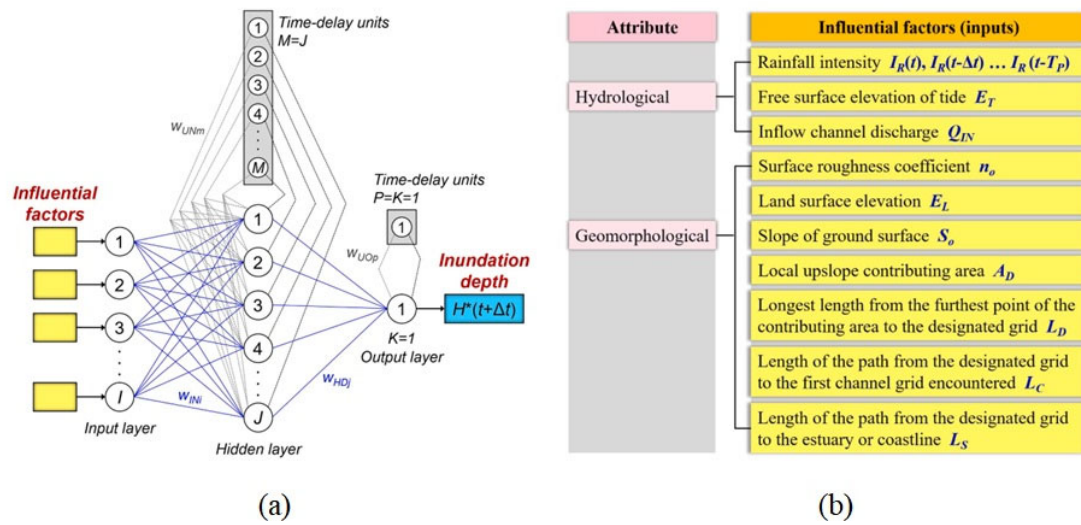


Figure 5. RNN model for predicting inundation depths [59]: (a) RNN model; (b) list of influential factors.

2.4. Summary

Figure 6 presents a comparative analysis of the performance of CNN/RNN models. It is evident that the majority of models exhibit R^2 and NSE values exceeding 0.95, showcasing outstanding hydrological forecasting capabilities. It can be observed that models enhanced by metaheuristic algorithms or operated under hybrid modes may have some potential for improving model performance.

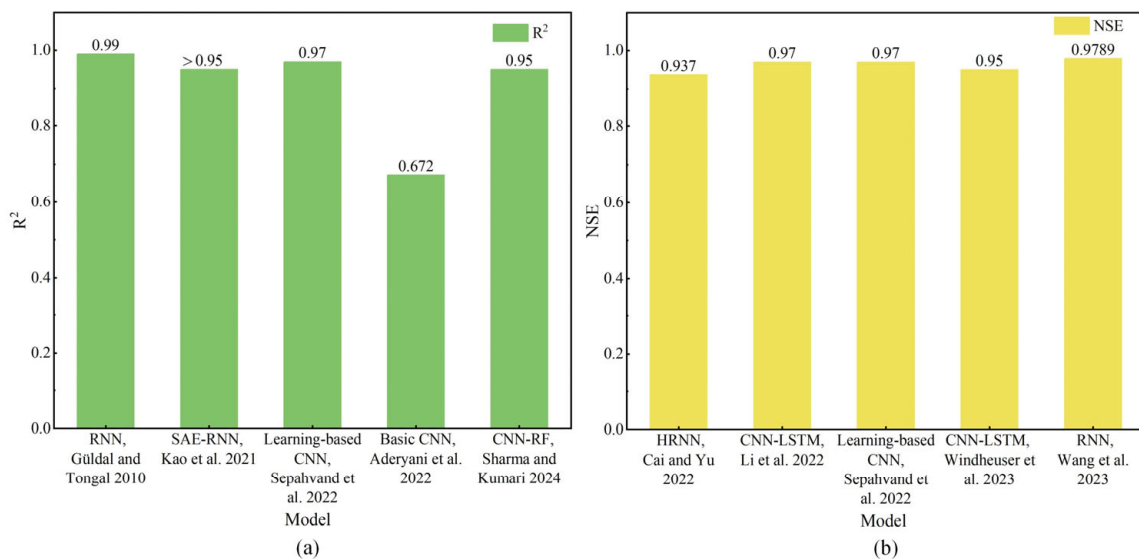


Figure 6. Performance comparisons between different CNN/RNN models [40,43–46,51,52,54,58]; (a) R^2 ; (b) NSE.

Drawing from the preceding literature review, Table 1 presents a comparison of various CNN/RNN models for hydrological forecasting. The CNN is good for image analyses, such as using the YOLOv2 framework for urban flood warning [41]. Its performance in time-series prediction is suboptimal. The regression models built using CNNs lack excellence in accuracy and often tackle relatively simple problems. In general, the model built using a one-dimensional CNN does not fully exploit the advantages of the CNN’s convolution. At this time, the integration of CNN and LSTM [43] techniques can bring out the advantages of each and improve the accuracy of the whole end-to-end model, which is valuable for

engineering applications. Unlike CNNs, there is a notable abundance of research in the literature focusing on RNN usage in hydrological prediction. Current research trends indicate that enhancing the RNN structure is an effective strategy to improve prediction accuracy, especially when addressing practical engineering challenges. Moreover, the complexity of engineering problems addressed by RNNs surpasses that of CNNs. For instance, RNNs can be combined with geographic information to improve the credibility and accuracy of hydrological prediction in a region [59].

Table 1. Comparison of different CNN/RNN models for hydrological forecasting.

Method	Minor Category	Authors	Problem and Difficulty Level	Improvement, Prediction Accuracy, and Computational Costs	Remarks
CNN	Learning-based CNN	Sepahvand et al. [40]	Hydrological infiltration modeling; medium	Applied innovation; improved accuracy over SVR; acceptable	Increased training time.
	YOLOv2 framework	Han et al. [41]	Flood management and flood warning; medium	Applied innovation; accuracy exceeded 90%; lengthy training	To be tested in practical engineering.
	CNN-LSTM	Windheuser et al. [43]	Flood stage prediction; hard	Integrated innovation; accuracy > 80%; lengthy training	Six-hour forecast accuracy needs improvement.
	Basic CNN	Aderyani et al. [46]	Rainfall forecasting; medium	Applied innovation; R ² not exceeding 0.7; acceptable	Prediction accuracy needs improvement.
RNN	Dynamic RNN	Coulibaly et al. [49]	Water resource prediction; medium	Local structural improvements; better than MARS; acceptable	Algorithmic advances beat traditional models.
	Basic RNN	Kim et al. [53]	Dam inflow prediction; medium	Applied innovation; prediction differences < 6%; acceptable	High-precision models enhance dam safety.
	BiRNN	Karbasi et al. [55]	Weekly reference evapotranspiration; medium	Local structural improvements; average R = 0.90; acceptable	Improves the CNN method and boosts hydrological forecasts.
	Basic RNN/BiRNN	Ayele et al. [56]	Dam inflow prediction; medium	Local structural improvements; close to GRU; acceptable	Accurate long-term predictions.
	RNN-RandExtreme	Wang et al. [57]	Extreme precipitation downscaling; hard	Integrated innovation; improved by 28.32%; acceptable	Enhances hydrological forecasting.
	RNN with geomorphological factors	Huang [59]	Flooding process; hard	Integrated innovation; MRE: 0.338 to 0.055; acceptable	Includes the coupling of geomorphological factors.

3. LSTM for Hydrological Forecasting

3.1. Principle of LSTM

LSTM, a specialized type of RNN, is adept at handling and forecasting significant events occurring over longer time intervals in time-series data. Unlike traditional RNNs, LSTM mitigates the issue of vanishing gradients, enabling it to effectively process both long- and short-term sequences. The conventional RNN architecture can be conceptualized as a “circuit” comprising multiple interconnected neurons. Each neuron receives input data, generates an output, and forwards it sequentially to the next neuron [60]. This structure can learn short-term dependencies on sequence data; RNNs struggle to perform well in processing long sequences due to issues such as gradient vanishing and explosion. LSTM can effectively solve long-sequence problems by introducing the concepts of memory cells, input gates, output gates, and forget gates (as shown in Figure 7). Memory cells are responsible for storing important information. The input gate determines whether to write the current input information into the memory cell, the forget gate determines whether to forget the information in the memory cell, and the output gate controls the utilization of information from the memory cells in generating current outputs. The manipulation of these gates enables LSTM to capture significant long-term dependencies in sequences and mitigate gradient-related problems. As a result, LSTM has successfully addressed the shortcomings of RNNs and become the most popular RNN currently [61,62], being successfully applied in many fields such as speech recognition, image description, and natural language processing.

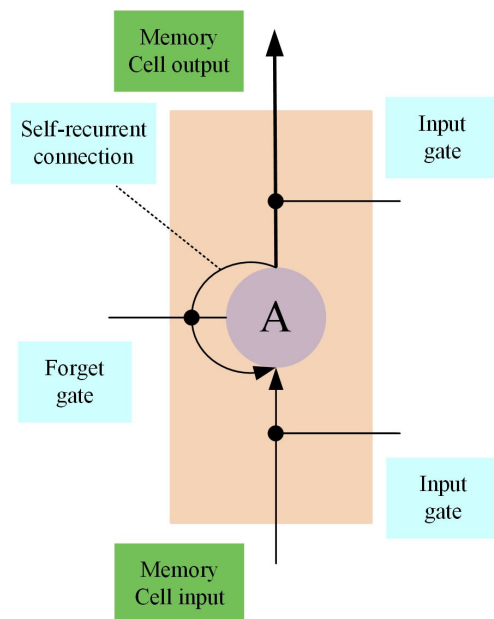


Figure 7. Structural diagram of the LSTM network.

3.2. Basic LSTM for Prediction

The LSTM network stands out as one of the most effective DL architectures for modeling dynamic hydrological variables [63]. When utilizing hydrological data, employing LSTM directly as a black-box model for hydrological forecasting has gained significant attention. In order to address the high randomness and non-statical nature of rainfall–runoff processes, Hu et al. [64] compared the predictive performance of ANN and LSTM models. By simulating the rainfall–runoff process of flood events in the Fenhe River from 1971 to 2013, it was found that both networks outperformed conceptual and physical models. Notably, the LSTM model exhibited superior performance compared to the ANN model (as illustrated in Figure 8), achieving R^2 and NSE values exceeding 0.9, respectively. The LSTM model demonstrated greater intelligence compared to the ANN model due to the implementation of a novel data-driven flood forecasting approach employing specialized forget gates. Although the first application of LSTM in hydrology seems to have been in 2017 [65], this research by Hu et al. is also one of the earlier studies to successfully utilize LSTM in hydrological prediction, and continues to be a highly cited paper (as of February 2024). Le et al. [66] proposed an LSTM neural network model for flood forecasting, utilizing daily discharge and rainfall as the input data. Flowrate predictions for one, two, and three days at the Huaping station yielded NSEs of 99%, 95%, and 87%, respectively. Their findings underscore the potential of applying LSTM models in hydrological contexts for the development and management of real-time flood warning systems. However, it is noted that the LSTM model only provided highly accurate forecasts at specific locations within the study area. Future endeavors should focus on integrating these models with meteorological models, such as rainfall forecasting models, to enhance long-term forecasting performance. DL techniques currently stand as the most accurate methods for making rainfall–runoff predictions. Hydrologists, however, are wary of the reliability and predictive accuracy of data-driven models based on deep learning when it comes to extrapolating or predicting extreme events. Frame et al. [67] explored this issue by utilizing an LSTM network along with a variant of an LSTM model. In comparison with the Sacramento model and the US National Water Model (NWM), the LSTM network and its mass-conserving counterpart demonstrated consistent accuracy in predicting extreme events, even in cases where such events were not represented in the training data. Based on meteorological data from the city of Jingdezhen from 2008 to 2018, Kang et al. [68] employed LSTM (nine significant input variables) to predict the precipitation in Jingdezhen, Jiangxi Province. Their experimental results showed that LSTM was more suitable for precipitation forecasting than classi-

cal statistical algorithms, such as the autoregressive moving-average model and MARS model, and machine learning algorithms, such as the ANN, SVM, and genetic algorithm approaches. The RMSE values for the training, validation, and test datasets of the best LSTM were 42.28 mm, 42.03 mm, and 41.72 mm, respectively. To improve the prediction accuracy of LSTM, this study preprocessed the data by removing input variables with weak correlation beforehand. Soil moisture is a key element of land surface hydrological processes, controlling surface energy and water balance. Its spatial distribution and seasonal variability can significantly impact weather and climate modeling over weekly to seasonal time scales. Fang and Shen [69] integrated the Soil Moisture Active and Passive (SMAP) technique with LSTM for the near-real-time forecasting of soil moisture. Their experimental results show that the median RMSE of model prediction performance decreased from 0.030 to 0.022 because of the SMAP integration. This underscores LSTM's adaptability and its ability to handle prediction tasks effectively, especially with the addition of hydrologically critical data, resulting in superior performance.

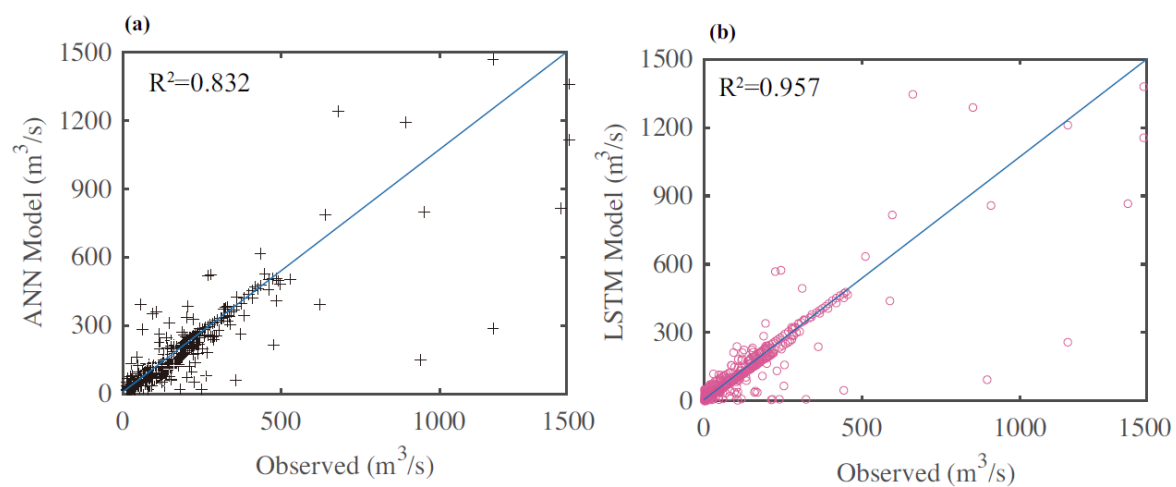


Figure 8. Rainfall–runoff prediction performance using ANN and LSTM models [64]: (a) ANN model; (b) LSTM model.

Many researchers consider utilizing LSTM as a surrogate model to reduce the computation time of distributed hydrological models. Gu et al. [70] developed a surrogate LSTM-based model that couples a self-organizing mapping (SOM) and K-means clustering algorithm with an LSTM as an alternative to the variable infiltration capacity (VIC) model. Their findings indicated that the runoff simulated by the surrogate model closely matched that of the VIC model in terms of NSEs at Yangcun station, as depicted in Figure 9. Moreover, employing the proxy model resulted in an over 97% reduction in the computation time. Modeling water flow in ungauged locations remains a significant hurdle in the field of hydrological forecasting. Arsenault et al. [71] undertook a comparative analysis between traditional zoning methods and the latest LSTM model. Their findings revealed that the LSTM model exceeded the performance of hydrological models in 93% to 97% of the watersheds, varying with the hydrological model used. Moreover, in up to 78% of the watersheds, the LSTM model achieved more accurate flow predictions in unmeasured catchments than the hydrological models, even when the latter were calibrated with targeted data. The LSTM model not only offers substantial improvements over conventional methodologies in predicting flows in ungauged catchments but also has the potential to significantly influence the future direction of zonalization research.

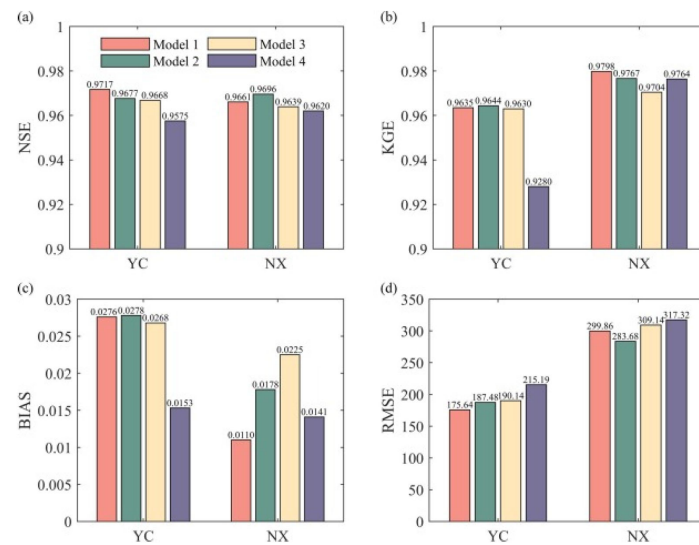


Figure 9. Performance evaluation comparing the fit quality between four surrogate model simulations and VIC simulation [70]: (a) NSE; (b) KGE; (c) BIAS; (d) RMSE (BIAS: relative bias; KGE: Kling–Gupta efficiency; YC: Yangcun station; NX: Nuxia station).

Both physics-based hydrological models and purely data-driven LSTM models have their own strengths and weaknesses: the former's performance is strongly influenced by the soundness of the model structure, with an inappropriate structure leading to very low model accuracy; the latter cannot demonstrate good generalization beyond the range of the training dataset. By effectively combining the two, complementary information is achieved to improve the simulation performance of the hybrid model. Lu et al. [72] conducted streamflow simulations in a data-scarce watershed using a hybrid Bayesian and machine learning model integrated with physical information. Their experimental results demonstrated that the LSTM model could reasonably predict daily runoff with NSEs higher than 0.8, while the hybrid model demonstrated improved out-of-distribution predictions with acceptable generalization accuracy. Koutsovili et al. [73] proposed an early flood monitoring and forecasting system based on a hybrid machine learning approach (LSTM), and their experimental results revealed that by combining the predictions obtained from the physical hydrological modeling system with those obtained from the LSTM, the accuracy of the flood predictions could be improved and an accurate flood forecast could be generated. This study highlights the effectiveness of combining physical and LSTM models to allow them to compensate for each other's limitations, thereby enhancing the interpretability and prediction accuracy of the fusion models.

3.3. Improved LSTM for Prediction

With the rapid advancement of the LSTM technique, improvements for the core components of LSTM and their successful application to hydrological forecasting have been emerging. Zou et al. [74] proposed residual LSTM (ResLSTM) for predicting flood probability as a multi-step model to overcome LSTM's gradient problems such as gradient vanishing and explosion. In addition, they introduced an autoregressive recurrent network into the proposed model. Their experimental results demonstrated that the time residual-based model was more accurate and robust than the original LSTM, GRU, and Time Feedforward Connections Simple Gate Recurrent Unit (TFC-SGRU) (depicted in Figure 10), and the accuracy of the peak flow predictions was close to 100% in the 90% prediction probability interval. This underscores the effectiveness of integrating residual and LSTM networks in mitigating gradient issues and enhancing model prediction accuracy. Xu et al. [75] developed a deep learning neural network model that integrates an LSTM network with particle swarm optimization (PSO) to predict the flooding process using rainfall and runoff data from all stations in a basin. The results indicated that the NSEs for the M-EIES, ANN,

PSO-ANN, LSTM, and PSO-LSTM models were 0.9211, 0.9423, 0.9461, 0.9761, and 0.9912, respectively, at a 1 h lead time. All models exhibited strong performance due to the short prediction interval. However, at a 12 h lead time, the NSE values decreased to 0.6922, 0.6534, 0.6596, 0.6842, and 0.7486, respectively, illustrating a reduction in simulation accuracy as the lead time extended. The PSO-LSTM model consistently maintained a higher level of prediction accuracy. Moreover, the integration of the PSO-LSTM model significantly enhanced the accuracy of short-term flood forecasting. Forghanparast et al. [76] performed intermittent runoff prediction for the headwaters of the Colorado River in Texas using DL algorithms and compared the prediction performance of four models, namely the extreme learning machine (ELM), CNN, LSTM, and Self-Attention LSTM (SA-LSTM) models. SA-LSTM was found to provide the best performance in capturing the extreme aspects of intermittent runoff flow rates (no-flow events and extreme floods) as the alternative and was found to be the most sophisticated tool among the four models. Also, Dai et al. [77] proposed a short-term water level prediction model (LSTM-seq2seq) based on the sequence-to-sequence approach. Their results revealed that the prediction accuracy of LSTM-seq2seq was higher than that of other models; for instance, the NSE values of the LSTM-seq2seq model consistently exceeded those of the LSTM-BP model by 0.02, with all values surpassing 0.72, and exhibited the fastest convergence process. The same findings were confirmed when forecasting the flow at multiple monitoring stations in the Humber River based on a hybrid LSTM model. Xiang et al. [78] introduced an LSTM-seq2seq model to predict hourly rainfall–runoff, conducting a comparative study at the Tripoli station in the upper Wapsipinicon River basin. Their study evaluated the performance of persistence, Lasso, SVR, LSTM, and LSTM-seq2seq models, with NSEs of 0.68, 0.68, 0.77, 0.72, and 0.85, respectively. Additionally, at the Independence and Anamosa stations, the 24 h persistence models showed high NSEs of 0.76 and 0.88, respectively. However, the LSTM-seq2seq model demonstrated superior performance with NSEs of 0.86 and 0.93 at these stations, outperforming both the persistence models and other comparative models. This study demonstrates that the LSTM-seq2seq model exhibits strong predictive capabilities and is an effective tool for enhancing the accuracy of short-term flood forecasts.

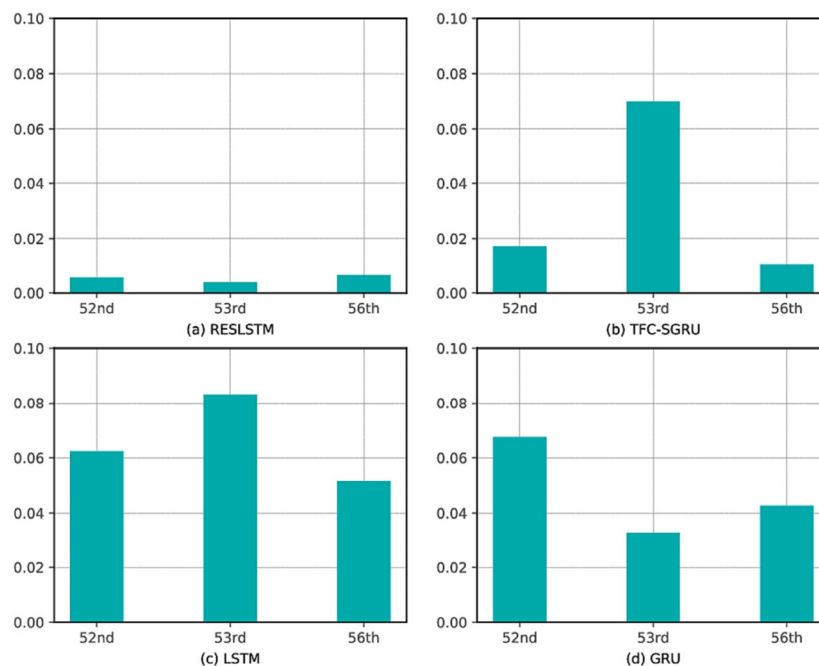


Figure 10. Comparison of flood peak prediction errors across three flood events for four different models [74]: (a) RESLSTM; (b) TFC-SGRU; (c) LSTM; (d) GRU.

Zhang et al. [79] evaluated the performance of LSTM, CNN-LSTM, convolutional LSTM (ConvLSTM), and spatiotemporal attention LSTM (STA-LSTM) models in flood forecasting and found that when the prediction time was greater than 6 h, the STA-LSTM model outperformed CNN-LSTM, ConvLSTM, and the basic LSTM model. This underscores the efficacy of integrating the attention mechanism with LSTM, leading to improved hydrological prediction accuracy and computational efficiency. Hu et al. [80] developed a framework integrating LSTM and reduced-order models (ROMs), termed LSTM-ROM, capable of representing the spatiotemporal distribution of floods. Evaluated using the Okushiri tsunami as a test case, the results achieved using LSTM-ROM closely aligned with those achieved using the full model (Fluidity) from a predictive analytics standpoint, with the CPU costs being reduced by three orders of magnitude when employing LSTM-ROM compared to the full model. Contemporary precipitation forecasting methods commonly overlook spatial autocorrelation characteristics, resulting in limited spatial information representation and extraction. Xu et al. [81] proposed a deformable convolution LSTM model considering spatial autocorrelation (DConvLSTM-SAC) for short-term precipitation forecasting. In their experiment, a continuous sequence of rainfall images spanning 3 h was utilized to forecast the subsequent 3 h period. The DConvLSTM-SAC model showed an average increase of 4.96% in R^2 and a decrease of 15.21% (9.01%) in the average RMSE (MAE). This DConvLSTM-SAC model provides an effective approach to address spatial autocorrelation in precipitation forecasting and exhibits promising performance in experiments. Cui et al. [82] proposed an encoder–decoder (ED) with an exogenous input (EDE) structure and integrated it with LSTM for multi-step-ahead flood forecasting. They compared and analyzed the performance of four models, namely the Xinanjiang (XAJ) hydrological model, LSTM with a recursive strategy, LSTM with a recursive ED (LSTM-RED), and LSTM-EDE, in multi-step-ahead flood forecasting. The results indicated that the EDE structure was better suited for long-term flood forecasting, outperforming the other models. However, attention should be given to the influence of the exogenous input accuracy on the LSTM-EDE model, particularly the gradual degradation of prediction performance with greater prediction horizons. Kao et al. [83] introduced a multi-step forecasting model using a long-short-term memory encoder–decoder (LSTM-ED) and evaluated its performance in multi-stage flood forecasting against that of a feedforward neural network-based encoder–decoder (FFNN-ED) model. The RMSE values of the LSTM-ED model at the $T + 2$, $T + 4$, and $T + 6$ forecast horizons were approximately 50% lower than those of the FFNN-ED model. Furthermore, the R^2 and NSE values for the LSTM-ED model exceeded 0.95 at all three horizons. These results demonstrate that the LSTM-ED model not only more effectively simulates the long-term dependencies between rainfall and runoff sequences but also provides more reliable and accurate forecasts compared to the FFNN-ED model. Han et al. [84] proposed a hybrid model based on a variational modal decomposition–LSTM–Breadth Learning System combination (VMD-LSTM-BLS) for the prediction of sea surface temperature (SST) in the East China Sea. Compared to those achieved with the benchmark SVM, RNN, and LSTM models, and the existing deep models, the maximum and minimum RMSE values were reduced by, respectively, 42.75% and 19.15%, which proves the advantages of the proposed VMD-LSTM-BLS hybrid model in SST prediction with relative stability and high efficiency. In addition, Yang et al. [85] combined temporal and spatial information and proposed a convolutional and fully connected LSTM (CFCC-LSTM)-based model for predicting future SST. Gauch et al. [86] introduced two multi-timescale LSTM (MTS-LSTM) models designed to simultaneously predict multiple temporal scales of rainfall–runoff within a single framework. The performance of these models was evaluated by comparing the differences in median NSE values and peak timing errors between the NWM and the MTS-LSTM models on both a daily and hourly basis. The results indicated median NSE discrepancies ranging from 0.11 to 0.16 for daily predictions and approximately 0.19 for hourly predictions. Specifically, the median peak timing error for the sMTS-LSTM model was about 3.5 h, in contrast to this being more than 6 h for the NWM. These findings demonstrate that the MTS-LSTM model not only achieves

a significantly higher NSE value compared to the NWM but also offers enhanced computational efficiency without sacrificing accuracy. Zhang et al. [87] employed a multi-layer convolutional LSTM model for predicting 3D ocean temperature. These studies underscore the significance of enhancing the internal structure of LSTM models, particularly through effective fusion with the predicted objects, to optimize model fitness and improve their prediction performance.

3.4. Summary

As depicted in Figure 11, the NSE values of these six models provide insights into their performance in data fitting. Notably, the PSO-LSTM model exhibited outstanding performance with an NSE value as high as 0.9912, indicating relatively minimal prediction errors and the strongest fitting capability. The NSE values of the remaining models all surpassed 0.8, indicating a high degree of fitting performance as well.

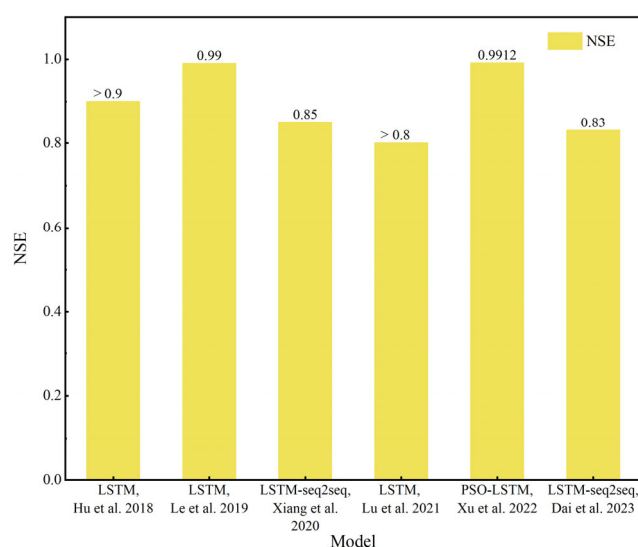


Figure 11. Comparison of NSEs of different LSTM models [64,66,72,75,77,78].

Based on the above literature review, Table 2 lists a comparison of different LSTM models for hydrological forecasting. There are also other studies that use these models, such as the basic LSTM model [46,88,89] and the improved LSTM model [90,91], for research on hydrological forecasting. Initially, primitive LSTM models demonstrated relatively strong prediction capabilities with minimal adjustments for hydrological forecasting tasks. Over time, the application of LSTM models has evolved from direct implementation (the black-box approach) to surrogate and hybrid physics models, expanding their scope and enhancing their prediction performance. While the direct application of LSTM is straightforward and requires minimal domain knowledge and modeling time, the interpretability of its models remains a concern. Basic LSTM models particularly demand extensive training data, and their performance heavily relies on data quantity, especially high-quality hydrological data. Integrating LSTM models with physical models enhances prediction accuracy and robustness. However, fusing models requires not only domain expertise but also skills in computer programming. To enhance the prediction performance, some scholars have fused popular deep network structures from other fields with LSTM models, such as residual modules in residual networks [74]. The inclusion of residual modules not only enhances the fitting of residual networks to achieve higher accuracy but also addresses the challenge of optimizing network training with deeper layers. Consequently, combining LSTM with residual networks deepens the network's architecture, mitigates the training complexity, and enhances the prediction performance. Moreover, attention mechanisms have been integrated into LSTM modeling to achieve further enhanced predictive capabilities in hydrological forecasting [76,77,79]. By introducing attention mechanisms, LSTM

models can be made to automatically learn and selectively focus on important information in the input data, improving the performance and generalization of the improved model. These studies underscore the potential for significant enhancements in LSTM model performance through the effective adaptation of cutting-edge DL advancements in hydrological forecasting, representing a promising avenue for future research.

Table 2. Comparison of different variants of LSTM for hydrological forecasting.

Method	Minor Category	Authors	Problem and Difficulty Level	Improvement, Prediction Accuracy, and Computational Costs	Remarks
Basic LSTM	LSTM	Hu et al. [64]	Rainfall–runoff; medium	Applied innovation; R ² exceeding 0.9; acceptable	An example of early LSTM use in hydrological prediction.
	Optimized LSTM	Kang et al. [68]	Precipitation; medium	Applied innovation; outperforms traditional statistics and ML; acceptable	Enhances rural precipitation predictions with sparse data.
	LSTM with SMAP	Fang and Shen [69]	Near-real-time forecasting of soil moisture; hard	Integrated innovation; outperforms LSTM sans SMAP; acceptable	Adding key hydrological data enhances the LSTM model.
	SOM + K-means + LSTM	Gu et al. [70]	VIC; very hard	Integrated innovation; close to the VIC model; acceptable	Saved > 97% computation time.
	Bayesian LSTM	Lu et al. [72]	Streamflow simulation; medium	Integrated innovation; desired performance; lengthy training	Enhances the fusion model's interpretability and accuracy.
	Vanilla LSTM	Koutsoveli et al. [73]	Early flood monitoring; hard	Integrated innovation; acceptable level; lengthy training	
Improved LSTM	ResLSTM	Zou et al. [74]	Flood probability; medium	Local structural improvements; surpasses original LSTM and GRU; acceptable	Residual LSTM integration mitigates gradient issues.
	SA-LSTM	Forghanparast et al. [76]	Intermittent runoff prediction; medium	Local structural improvements; achieved the best performance among the four models studied; acceptable	Model uses attention mechanisms for accuracy.
	LSTM-seq2seq	Dai et al. [77]	Short-term water level prediction; medium	Local structural improvements; NSE = 0.83; acceptable	
	LSTM-EDE	Cui et al. [82]	Multi-step-ahead flood forecasting; hard	Local structural improvements; more suitable for long-term flood forecasting; acceptable	Model performance degrades with longer prediction periods.
	VMD-LSTM-BLS	Han et al. [84]	SST prediction; medium	Local structural improvements; RMSE reduction: max 42.75%, min 19.15%; acceptable	Signal decomposition integration enhances LSTM SST accuracy.
	Multi-layer convolutional LSTM	Zhang et al. [87]	SST prediction; medium	Local structural improvements; predicted data are generally accurate; acceptable	Links temperature time series with spatial seawater data.

4. GRUs and Others for Hydrological Forecasting

4.1. Principle of GRUs and Others

The GRU, akin to LSTM, is a type of RNN designed to address challenges such as long-term memory retention and gradient vanishing during backpropagation [92,93]. Compared to LSTM, a GRU exhibits notable performance and is easier to train, significantly enhancing the training efficiency. This advantage stems from the similarity of the GRU's input and output structure to that of standard RNNs, coupled with its LSTM-like internal processing. Although a GRU lacks LSTM's gate control and features fewer parameters, it can perform comparably to LSTM. A generative adversarial network (GAN) is a DL model that consists of two main components: a generator and a discriminator [94,95]. The task of the generator is to receive random noise as its input and generate samples similar to real data. The task of the discriminator is to distinguish between real data and fake data generated by the

generator, and these networks learn through adversarial competition. Hydrological data, such as rainfall data from outdoor observation stations, are often incomplete due to various uncontrollable factors, hindering their direct use for prediction tasks. Therefore, GANs have a strong data generation ability through the game balance between the generator and discriminator, and can fully utilize existing data for training and learning, thereby generating the required data. Additionally, residual networks (ResNets), graph neural networks (GNNs), and other architectures are gaining traction among researchers.

4.2. GRUs for Prediction

Zou et al. [74] combined autoregressive recursive networks with a GRU to address the nonlinearity problem of natural hydrological characteristics in watersheds and achieved hydrological predictions for the Passaic and Ramapo River basins in the United States. Their findings revealed that the peak flow accuracy fell within a 90% prediction probability interval, with predictions approaching 100%, underscoring the model's robust adaptability to flood uncertainty. In a separate study, Xie et al. [96] adopted two networks, a GRU and an LSTM model, to carry out a hydrological simulation of green roofs. Their results confirmed that as the length of the time window (the memory length, i.e., the time step of input data) increased, both models achieved a higher overall prediction accuracy, suggesting the utility of GRUs and LSTM in modeling hydrological processes on green roofs. Tabas and Samadi et al. [97] combined the Monte Carlo dropout (MC-dropout) uncertainty technique in Bayesian inference with GRU, LSTM, and RNN methods to quantitatively model rainfall–runoff in a mixed urban and rural coastal watershed in North Carolina, USA. The simulation results showed that the GRU and LSTM methods had significant advantages compared to previous classical models, as depicted in Figure 12. If floodwater level data can be predicted, economic and human losses caused by floods can be alleviated. A water level prediction model incorporating LSTM-GRU was proposed by Cho et al. [98]. Optimal results were achieved when the input data included both the LSTM-GRU model and meteorological data from an automated weather observation system. The experimental results demonstrated that the LSTM-GRU model attained a mean square error (MSE) of 3.92, an NSE of 0.942, and an MAE of 2.22, all of which were the highest among all scenarios. By comprehensively considering meteorological and water level data, this model effectively predicted flood risks with high accuracy and practicality. Future research could further optimize this model to enhance its applicability and reliability. Zhang et al. [99] employed a spatiotemporal attention–gated recurrent unit (STA-GRU) model for flood prediction to enhance computational efficiency. When the dataset underwent preprocessing with lag time, the R^2 value of the STA-GRU model increased from 0.6181 to 0.7232, the RMSE decreased from 0.1220 to 0.1039, and the MAE reduced from 0.0625 to 0.0534. These results indicate the enhanced predictive performance of the STA-GRU model. This improvement is attributed to the superior capability of GRUs in handling temporal data. These findings hold significant implications for enhancing the efficiency and accuracy of flood prediction. Kilinc et al. [100] proposed combining the grey wolf optimization (GWO) algorithm with a GRU for predicting daily flow data in the Seyhan basin. Their study yielded an R^2 of 0.9127, an RMSE of 82.9352 cubic meters per second (m^3/s), an MAE of 85.9337 m^3/s , and a MAPE of 62.4796 m^3/s for the GWO-GRU hybrid model. The results obtained with the GWO-GRU hybrid model significantly enhanced the accuracy of flow prediction, with the insights and data derived from its flow forecasting being particularly valuable for designing water infrastructure, flood alert systems, and more effective water management. Chhetri et al. [101] proposed a rainfall forecasting model based on bidirectional long short-term memory (BLSTM-GRU). Daily weather parameter records from the Bhutan region spanning from 1997 to 2017 were utilized as the research dataset. Their results indicated an R^2 of 0.87 for BLSTM-GRU. Additionally, its MSE was 0.007, which was 41.1% higher than that of LSTM. This LSTM-GRU model demonstrates a high level of accuracy and predictive capability in rainfall forecasting, which may hold practical significance for meteorological prediction and related domains. In addition, using the MC-dropout

technique, the inherent input data Gaussian noise term was applied to the RNN layer, implicitly reducing overfitting and significantly improving the predicted log likelihood. Guo et al. [102] combined ensemble learning methods with residual correction to propose a hybrid hydrological prediction model for mountainous areas. They incorporated the predicted outputs of three models, namely an encoder–decoder GRU (ED-GRU), an encode–decode LSTM (ED-LSTM) model, and a convolutional neural network LSTM combination (CNN-LSTM), into the classification gradient-boosting regression (CGBR) model, solving the highly nonlinear relationship between the model’s input and output. The results showed that the proposed model had a good predictive ability in predicting reservoir peak and total inflow data. Compared with the three DL models, the proposed model achieved an average performance improvement of 66.2% and also performed well on storm events with multiple peak water levels. In addition, the emergence of the bidirectional GRU has further improved the predictive performance of its model [103–105] and has been applied in some hydrological forecasting research [106].

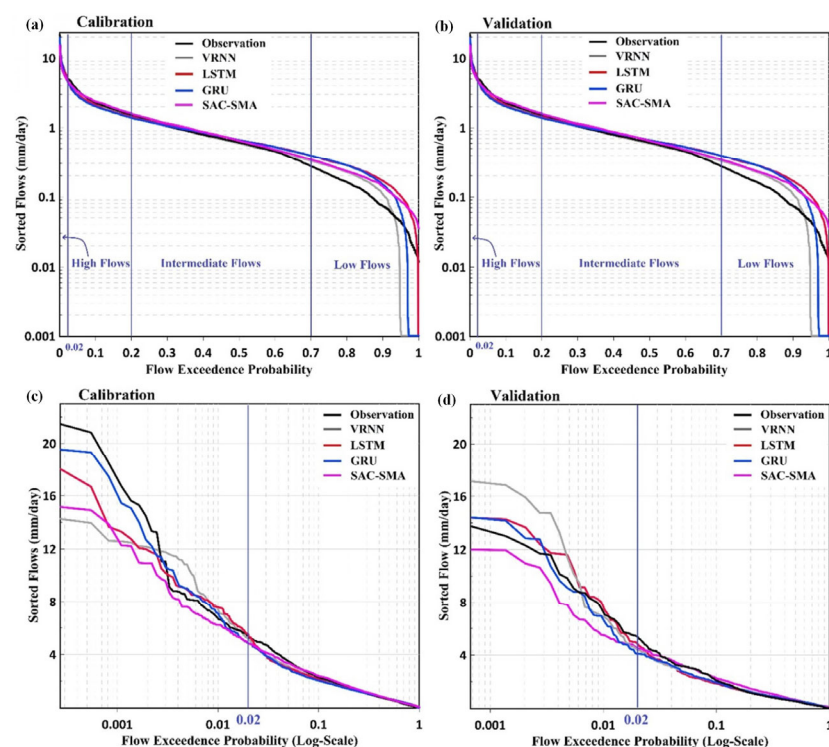


Figure 12. Comparative analysis of daily streamflow simulation performance using four modeling methods [97]: (a) calibration; (b) validation; (c) calibration (Log-Scale); (d) validation (Log-Scale).

4.3. Other Methods for Prediction

Li et al. [107] fused a GAN with a fuzzy inference model for predicting multidimensional incomplete hydrological big data. In the proposed fusion model, the GAN was utilized to generate data to complete the incomplete hydrological data; the fuzzy inference model was used for rainfall–runoff prediction. The experimental results indicated that combining GAN and fuzzy inference modeling yielded satisfactory prediction results, particularly in the rainy season. Hofmann and Schüttrumpf [108] have developed a floodGAN model for predicting pluvial floods caused by nonlinear, spatially heterogeneous rainfall events. The performance and accuracy of floodGAN were evaluated through multiple tests using synthetic events and historical rainfall events. The average R^2 values of the test datasets ranged from 0.80 to 0.85. This floodGAN model bridges the gap between detailed flood modeling and real-time applications such as end-to-end warning systems. Lago et al. [109] introduced a method termed the conditional generative adversarial network–Flood (cGAN-Flood) method, utilizing a cGAN for flood prediction within catchment areas

not included in the training process. Across the four rainfall events tested, the R^2 values exceeded 0.7 for each event. These findings demonstrate the robust predictive performance of the cGAN-Flood method concerning flood location and water depth. Given its computational efficiency and accuracy, cGAN-Flood emerges as a viable modeling solution for large-scale basin flood forecasting. Laloy et al. [110] utilized a spatial GAN for groundwater modeling, and their research demonstrated the effectiveness of synthetic inversion involving two-dimensional steady-state flow and three-dimensional transient hydraulic fault scanning. In addition, several other researchers have made useful summaries of the application of GANs and their various improved algorithms in hydrological prediction [111]. Some other DL networks have also received attention from relevant scholars. Ren et al. [112] proposed a novel hybrid KNN-FWA-ELM method, integrating the k-nearest neighbor (KNN) technique, the fireworks algorithm (FWA), and an extreme learning machine (ELM) for flood prediction in a loess region's medium and small watersheds. Their study focused on the Gedong basin in the western loess region of Shaanxi, analyzing surface changes and flood characteristics. The results indicated that the R^2 of the KNN-FWA-ELM model was 0.86, which was 0.04 higher than that of the ELM model. Additionally, the KNN-FWA-ELM model exhibited superior simulation performance and higher accuracy in flood prediction, with a qualification rate 17.39% higher than that of the ELM model. While the hybrid model achieved favorable flood forecasting results in medium and small watersheds of the loess region, it had drawbacks such as the need for manual determination of the hidden node numbers. Zhang [113] employed a residual network (ResNet) to process multitemporal remote-sensing imagery and predict changes in Greenland glacier fronts and found that the predictions were favorable. Spatial autocorrelation analysis improves flood warnings by refining spatial data patterns for more accurate predictions. Zhou et al. [114] introduced an ML-based urban flood warning system. Spatial autocorrelation analysis, using Moran's I , confirmed a significant positive spatial correlation between rainfall (at a 95% confidence level) and inundation points. Models employing gradient-boosting decision tree, SVM, and backpropagation neural network algorithms were constructed for predicting this rainfall–inundation relationship, with the gradient-boosting decision tree approach showing the lowest RMSE (0.001 m) in predicting the inundation depth. This integrated approach enhances the accuracy and reliability of urban flood warning systems by combining spatial autocorrelation analysis with model construction. Bui et al. [115] conducted a comparative study of various innovative hybrid models that integrate swarm intelligence algorithms with deep learning neural networks for flood sensitivity mapping. These models leverage recently developed swarm intelligence optimization algorithms that emulate the behaviors of gray wolves, social spiders, and grasshoppers to fine-tune deep learning neural networks for flood sensitivity mapping. The stability performance of these models was assessed using the area under the receiver operating characteristic curve (AUC) as a metric, where higher AUC values indicate greater model robustness. The study found that SSO (AUC = 97.003%), the GOA (AUC = 96.798%), and GWO (AUC = 96.751%) exhibited notable stability. The validation of the stability of the GWO algorithm, SSO algorithm, and GOA, which are inspired by animal behavior, enhanced this modeling approach and informed similar research efforts in other fields. Multi-scale feature representation is vital for estimating floodwater surface displacement, providing comprehensive monitoring and predictive data, thus enhancing flood risk management. Chew et al. [116] developed a multi-scale homogeneous deep neural network (MHDNN-UPC) to predict water surface displacement, representing flood scenarios induced by peak flow conditions. The MHDNN-UPC method incorporates features of different scales into flood prediction modeling and enhances computational performance through unified parallel computing. Compared to other traditional models, this model demonstrated an average increase in prediction accuracy of 10%, along with improved computational performance and the execution capability of the UPC component. MHDNN-UPC achieves enhanced computational efficiency while improving the forecast accuracy. In addition, GNNs have

also been applied to hydrological prediction [117,118]. For example, the GNN framework proposed by Zhao et al. [117] can effectively predict a river's flow during its initial stage.

4.4. Summary

As shown in Figure 13, the GWO-GRU model achieves the highest R^2 value of 0.9127, indicating its strong capability in explaining the variability of the data and demonstrating good predictive performance. The BLSTM-GRU model performs relatively well with an R^2 value of 0.87. The remaining models also exhibit reasonably accurate predictive capabilities, with the cGAN-Flood model showing a slightly lower performance due to the larger volume of data it handles.

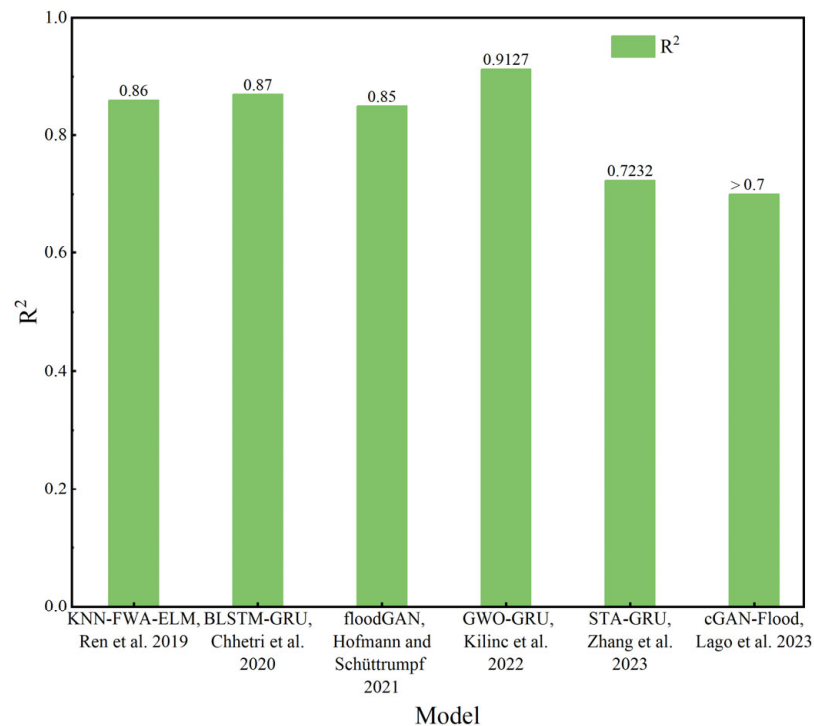


Figure 13. Comparison of R^2 values between GRU models and other models [99–101,108,109,112].

Based on the above literature review, Table 3 lists a comparison of different variants of GRUs or other models for hydrological forecasting. Based on the existing literature, the application of GRUs in hydrological forecasting occurs much less than that of LSTM. The performance of the GRU is comparable to that of LSTM on medium-scale to large-scale data, while the GRU and LSTM methods have their own advantages and disadvantages in processing ultra-large data [119–121]. The GRU has a shorter processing time and is suitable for real-time requirements. Although LSTM exhibits slightly higher accuracy, it is notably time-consuming. This elucidates a significant reason why GRU applications garner less attention than LSTM in hydrological forecasting. At present, the application of GRUs in hydrological forecasting in the literature is mainly based on basic algorithms [74,94,95], although there are also many improved versions of the GRU, such as the bidirectional GRU [122,123] or versions with added attention mechanisms [124,125]. Other types of DL algorithms, such as GANs, ResNets, and GNNs, have been utilized in hydrological forecasting, yielding more satisfactory prediction outcomes [107,110,113,117,118]. For example, the emergence of the GAN is significant for dealing with missing hydrological data. However, the number of related research works on these topics remains limited, particularly in terms of the thorough adaptation of algorithms to this research context.

Table 3. Comparison of different variants of GRU models or other models for hydrological forecasting.

Method	Minor Category	Authors	Problem and Difficulty Level	Improvement, Prediction Accuracy, and Computational Costs	Remarks
GRU	Basic GRU	Zou et al. [74]	Flood probability; medium	Local structural improvements; acceptable; acceptable Applied	Easily implemented; lowers threshold.
	Basic GRU	Xie et al. [96]	Hydrological simulation of green roofs; medium	innovation; higher overall prediction accuracy; acceptable	Finds optimal parameters for high accuracy.
	GRU+ MC-dropout	Tabas and Samadi et al. [97]	Streamflow simulation; hard	Local structural improvements; acceptable; acceptable	Combining models with noise reduces uncertainty.
	GRU + CGBR	Guo et al. [102]	Hourly inflow for reservoirs at mountain catchments; hard	Integrated innovation; acceptable; acceptable	Model performance depends on the dataset's quality.
Others	GAN	Li et al. [107]	Rainfall–runoff prediction; hard	Integrated innovation; acceptable; acceptable Applied	GANs generate data better than random forest models.
	GAN	Laloy et al. [110]	Groundwater modeling; very hard	innovation; acceptable; acceptable	Spatial GANs require fewer training images.
	ResNet	Zhang [113]	Changes in Greenland glaciers; hard	Integrated innovation; acceptable; medium	Assess generalizability and robustness for wider use.

5. Discussion

5.1. DL vs. Traditional ML and Physical Models

In the field of engineering, physical models are considered to be useful in understanding the physical mechanisms inherent in objective phenomena [126–128]. In general, the accuracy of physical model predictions depends on the physical properties of the model, the initial conditions of the watershed, and the spatial and temporal resolution of the predictor and predictor variables. This not only makes it necessary for the relevant researchers to have expertise and experience in the model, but also requires a professional background in industries such as mathematics and computers. Further, the associated computational process is very resource- and time-consuming. It is also a challenge to realize highly accurate hydrological forecasts in a timely manner with limited time and resources. In addition, it is difficult to migrate the physical models built for specific scenarios to other areas, which further raises the threshold for their popularization and application.

DL and traditional machine learning are two important branches in the field of machine learning, and they differ significantly in their hydrological forecasting applications. Traditional machine learning usually requires manual feature engineering, i.e., extracting meaningful features from raw hydrological data. DL, on the other hand, is able to automatically learn features through multi-layer neural networks to obtain higher-level representations from raw data. DL's capacity for end-to-end applications reduces the computational demands for hydrology researchers. This means that feature engineering no

longer needs to be executed manually to achieve better hydrological forecasts. Traditional machine learning operates effectively with smaller datasets [18,129]. DL requires relatively large amounts of data, especially in deep neural networks [130]. Compared with traditional machine learning, DL is able to automatically learn features from raw data, which can result in richer information and higher-level feature representations, thus improving model performance. Consequently, with the continuous accumulation of hydrological data, DL's application in hydrological forecasting is broadening, encompassing runoff prediction, flood forecasting, reservoir level prediction, groundwater level prediction, and more.

A comparison of DL, traditional ML, and physical models for hydrological forecasting is listed in Table 4. For example, physical models typically require a significant amount of computation to achieve sufficient progress and are not yet easy to transplant to new scenarios. However, their advantage is their good interpretability, as they are modeled based on actual hydrological conditions. Consequently, all three types of models coexist in current hydrological forecasting research. However, the focus of research on hydrological forecasting models is gradually shifting from physical models to traditional machine learning and DL. This trend is particularly evident, especially given the recent rapid advancements in artificial intelligence.

Table 4. Comparison of DL, traditional ML, and physical models for hydrological forecasting.

Methods	Difficulty of Application	Computing Time	Replicability	Interpretability
Physical models	Hard	Long	Very hard	Yes
Traditional ML	Middle	Short	Hard	Partially
DL	Easy	Acceptable level	Acceptable level	No

5.2. Comparison of Various DL Algorithms

Generally speaking, CNN deep learning models are mainly used for understanding images and other aspects [25,130,131], and their strength is not in predicting data series. Therefore, the application of CNNs is not very common in the existing hydrological forecasting literature. However, as satellite/aerial photography methods for obtaining optical and remote sensing images become increasingly economical, CNN models can be used to establish a certain correlation between these large-scale images and hydrological forecasting, such as for predicting urban waterlogging [41]. In this way, the advantages of CNNs will be fully utilized in hydrological forecasting.

RNN deep learning models have been applied in hydrological forecasting, such as for analyzing water resources, dam inflow, flooding processes, extreme precipitation, and others. Although RNNs can predict hydrological time-series data, they encounter challenges with long sequence data. This is due to the problem of vanishing/exploding gradients in RNNs during their training [132,133], rendering these models difficult to train or unable to converge. Furthermore, due to the vanishing gradient, RNNs find it difficult to capture long-term dependencies when processing long sequences, and can only effectively utilize shorter contextual information. In addition, the calculation process of an RNN is based on time-step expansion, and each time step needs to be calculated sequentially, resulting in low computational efficiency, particularly with long sequences. Therefore, for long-term hydrological forecasting, the RNN model needs further improvement to enhance its prediction accuracy.

In hydrological forecasting, LSTM deep learning models are widely used, including the basic LSTM model and various improved versions [64,68,84,87]. This is due to LSTM's ability to circumvent the critical drawback of a traditional RNN [134–136], making it more user-friendly for processing hydrological sequence data, especially for long sequence data. Based on existing research, the LSTM model and its various improved versions run well under normal conditions, but may fail in extreme situations. In order to achieve better results, it is necessary to strengthen the collection of high-quality, long-sequence hydrological training datasets. This entails furnishing extensive historical data with consistent statistical

features, orchestrating the development of high-resolution observations, and conducting thorough data analyses for both training and testing purposes.

A GRU can be seen as a simplified version of LSTM, as it combines cellular and hidden states into one state and uses update and reset gates for control [137,138]. Therefore, GRUs solve the problem of vanishing gradients by using gate mechanisms to control the flow of information, thus enabling better learning of long-term dependencies. In contrast to LSTM, a GRU possesses fewer parameters, resulting in faster training and reduced susceptibility to overfitting. However, in tasks that require modeling complex sequential dependencies, GRUs may not exhibit a performance comparable to that of LSTM, contributing to their relatively limited presence in hydrological forecasting research compared to LSTM. In addition, GRUs may need to make some adjustments to the hyperparameters to achieve optimal performance, which poses a challenge for researchers and requires a certain foundational knowledge in computer applications. Alternative DL models, including ResNets, GANs, and GNNs, are typically integrated with other frameworks and seldom serve as the primary component for conducting hydrological forecasting tasks. For example, GANs can generate missing hydrological data based on the trend of historical data changes. Thus, Table 5 presents a comparison of the CNN, RNN, LSTM, GRU, and other models for hydrological forecasting.

Table 5. Comparison of CNN, RNN, LSTM, GRU and other models for hydrological forecasting.

Methods	Number of Appearances in the Literature	Difficulty of Application	Accuracy	Complexity
CNN	Less	Easy	Acceptable level	Acceptable level
RNN	Less	Middle	Relatively satisfactory	Simple
LSTM	More	Middle	Relatively perfect	Middle
GRU	Less	Middle	Relatively satisfactory	Simple
ResNet	Much less	Easy	---	Middle
GAN	Much less	Hard	---	Huge
GNN	Much less	Hard	---	Middle

Note(s): More: >30 articles; less: 20–30 articles; much less: <20 articles. Complexity indicators: framework, parameter quantity, and training time.

5.3. Advantages and Disadvantages of Hybrid Models

Figure 14 illustrates the strengths and weaknesses of DL, physical, and hybrid models for hydrological forecasting. In contrast to physical models, the mapping between the input and output in DL models does not require consideration of actual physical processes, which simplifies the difficulty of building these models and accelerates research progress for more hydrological researchers. By successfully building an end-to-end model, automatic fitting of the nonlinear relationship between the input and output becomes feasible. While this model type boasts a low complexity, it also presents a challenging issue to address (i.e., the lack of interpretability), given that DL models operate as black-box methods. For example, in the context of flood predictions within crucial river basins, which encompasses numerous factors such as personnel safety, property transfer, disease transmission, and road network damage, enhancing the interpretability and credibility of hydrological forecasting can facilitate more informed decision making among managers. In order to improve the interpretability of DL models, Konapala et al. [72,139] created various hybrid models that combine different forms of hydrological information with LSTM networks in different ways. For example, some of the data trained in LSTM networks come from additional data/information from physics-based models. This approach can address the limitation of purely data-driven LSTM models in generalizing beyond the training range due to insufficient historical observations, thereby enhancing the accuracy of hydrological forecasting. Additionally, other researchers have also combined different DL models with physical models to improve the accuracy and interpretability of these models [97,140]. However, the current method of combining DL and physical models for hydrological forecasting still

relies on passive learning. This indicates that DL models exist in a non-active learning state for prediction since they cannot be trained without actual simulation. As of right now, the AlphaFold2 approach correctly predicts 98.5% of human protein structures by integrating biological and physical knowledge on protein structures into the design of DL algorithms [15]. This makes the suggested model both interpretable and capable of active learning. In a similar vein, this suggested model may independently search for and assess the tertiary structure of RNA and achieve the highest prediction accuracy by combining geometric topology with DL algorithms [141]. Naturally, with the rise in model autonomy and interpretability, complexity has also increased, posing challenges in the development of pertinent research. To enhance the autonomy, intelligence, and interpretability of models, the current trend in hydrological forecasting research involves integrating DL with physical simulations, drawing upon successful experiences from fluid mechanics [142] and biology [15,141].

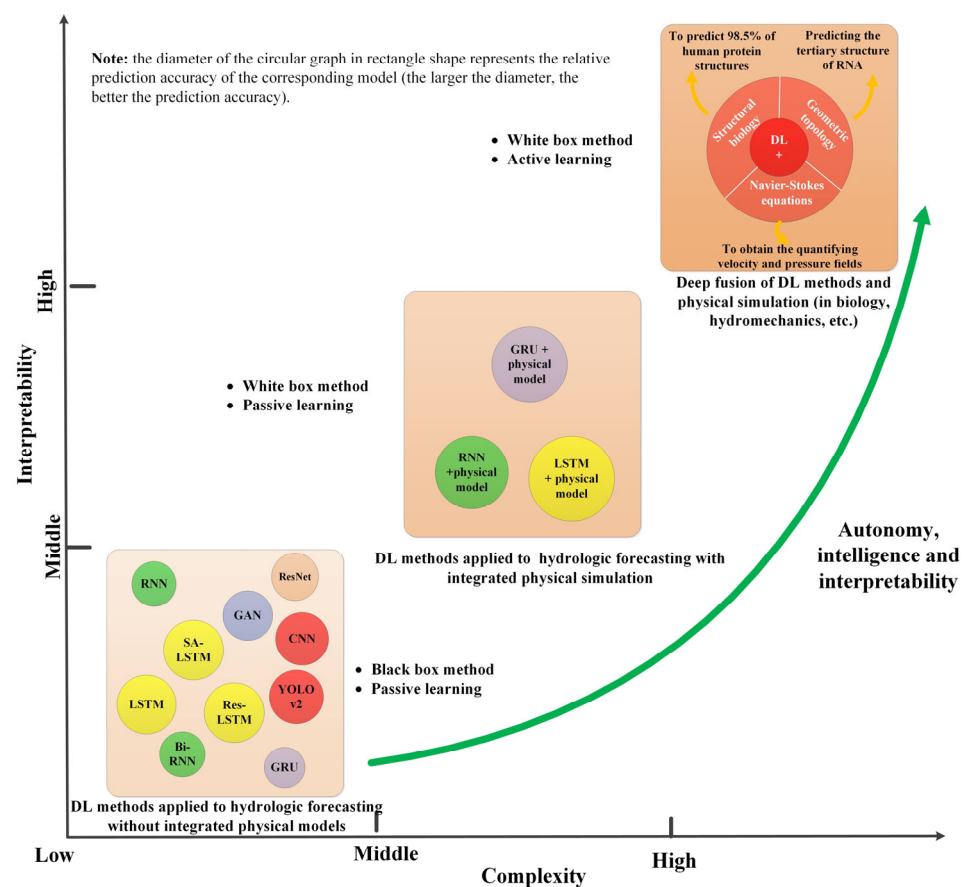


Figure 14. Advantages and disadvantages of DL, physical, and hybrid models for hydrological forecasting.

5.4. Challenges in the Application of DL Models

Spatial autocorrelation is a major challenge in hydrology, addressed using widely studied traditional statistical methods. For instance, Poisson regression with feature vector space filtering is used to simulate flood risks at hydrological stations, and grid data are used for spatiotemporal autocorrelation analyses of extreme precipitation events [143,144]. DL methods, like enhanced LSTM models, have been attempted for short-term precipitation forecasting. Deepening our understanding of spatial heterogeneity aids in effectively identifying hydrological features and issues, thereby improving the accuracy and applicability of hydrological models. For example, statistical analysis methods have been utilized to study rainfall spatial heterogeneity in urban areas [145]. However, hydrological research on DL models predominantly focuses on model design, algorithm optimization, and performance

evaluation, with limited exploration of spatial heterogeneity. Multi-scale feature representation is essential in hydrological prediction for capturing system complexity and variability, improving model adaptability and prediction accuracy. Early techniques focused on regionalization but have since expanded to broader scales and climate systems [146]. DL models excel at automatically learning features from data, handling multi-scale features effectively. For instance, multi-scale homogeneous deep neural networks can predict water surface displacement during peak flow. While current research on multi-scale features is limited, DL's increasing application in hydrology is expected to drive further advancements, enhancing the accuracy of prediction models.

6. Outlooks

With the latest developments in computational technology, data-driven machine learning models, especially deep learning models, have made tremendous progress in hydrological forecasting. For example, they show great potential in re-simulating streamflow and capturing rainfall–runoff relationships for a given watershed, which have traditionally been carried out using process-based physical models. Thus, with the help of DL models, hydrological forecasting is made less difficult and the prediction performance is more stable and less costly. This area has garnered increasing attention from researchers. Therefore, based on the literature review in this study, the future directions of hydrological forecasting based on DL models are as follows.

- (1) CNN models continue to be relevant in hydrological forecasting and need to be utilized for their unique advantages in handling massive image data. Moving forward, CNNs and improved CNN models can be integrated with other deep models to achieve hydrological data analyses that not only include time-series data (short-/medium-/long-term) but also encompass time-series image data (optical/remote sensing), which can further improve the prediction performance of these models. The RNN model, as a basic time-series prediction method, is constrained by its structure, and it needs to be further improved to achieve more applications in the field of hydrological prediction.
- (2) With the deepening of research, there will be a tendency in the future to design more complex deep learning models to better capture the inherent coupling relationships in hydrological forecasting sequence data. New variants and improved model structures based on LSTM continue to emerge, such as improved LSTM variants, more attention mechanisms, more parallel processing, and more effective weight sharing. This enables the design of deeper and more effective LSTM structures, utilizing GPUs and TPUs for more effective parallel processing, thereby improving the training and inference speed of the model.
- (3) Both GRUs and GNNs are expected to achieve greater breakthroughs in the future, especially in the field of hydrological forecasting. For GRUs, attention mechanisms and improved gating mechanisms can be introduced to better handle hydrological sequences of variable length and their complex coupling relationships. For GNNs, the efficiency and performance of processing large-scale graph data can be improved by introducing new graph convolution operators and developing efficient graph sampling strategies.
- (4) The combination of physical properties and deep learning helps to explain the working principle of the model and improve its interpretability, which is crucial for critical hydrological forecasting applications and helps to enhance trust and acceptance of the model's results. In the future, hybrid models should also have an active learning ability and a self-iterative evolution ability, and continuously improve hydrological forecasting performance.
- (5) Spatial autocorrelation challenges DL models due to data and weight matrix issues. Future solutions may include innovative model structures and feature methods. Ensuring the model's applicability across different regions encounters challenges such as data bias, imbalance, and the integration of spatial information, reflecting spatial

heterogeneity. Overcoming these obstacles may require model optimization, data expansion, and interdisciplinary collaboration. Multi-scale feature representation involves scale matching and computational costs. Future solutions may focus on improving model performance and applicability to address this issue.

Author Contributions: X.Z. and H.W. wrote the first draft. Y.X., M.B. and H.W. carried out the formal analyses. X.Z., H.R. and W.M. completed most of the of the literature review. S.D. and W.M. proposed the study's concept and methodology, and acquired the funding. X.Z. and H.W. contributed equally to this review article. All authors have read and agreed to the published version of the manuscript.

Funding: This work was supported by the Guangdong Basic and Applied Basic Research Foundation (No. 2022A1515140066) and by the Henan Provincial key scientific and technological project (No. 222102220011).

Conflicts of Interest: Author Hui Rao was employed by the company Wuhan Jianglai measuring Equipment Co., LTD. The remaining authors declare that the research was conducted in the absence of any commercial or financial relationships that could be construed as a potential conflict of interest.

References

1. Tellman, B.; Sullivan, J.A.; Kuhn, C.; Kettner, A.J.; Doyle, C.S.; Brakenridge, G.R.; Erickson, T.A.; Slayback, D.A. Satellite Imaging Reveals Increased Proportion of Population Exposed to Floods. *Nature* **2021**, *596*, 80–86. [CrossRef]
2. Oyelakin, R.; Yang, W.; Krebs, P. Analysing Urban Flooding Risk with CMIP5 and CMIP6 Climate Projections. *Water* **2024**, *16*, 474. [CrossRef]
3. Wang, Z.; Wang, H.; Huang, J.; Kang, J.; Han, D. Analysis of the Public Flood Risk Perception in a Flood-Prone City: The Case of Jingdezhen City in China. *Water* **2018**, *10*, 1577. [CrossRef]
4. Available online: <https://www.huxiu.com/article/446118.html> (accessed on 24 March 2024).
5. Jongman, B. The Fraction of the Global Population at Risk of Floods Is Growing. *Nature* **2021**, *596*, 37–38. [CrossRef]
6. Global Flood Database. Available online: <https://global-flood-database.cloudtostreet.ai/> (accessed on 28 March 2024).
7. He, J.; Zhang, L.; Xiao, T.; Wang, H.; Luo, H. Deep Learning Enables Super-Resolution Hydrodynamic Flooding Process Modeling under Spatiotemporally Varying Rainstorms. *Water Res.* **2023**, *239*, 120057. [CrossRef]
8. Libya | History, People, Map, & Government | Britannica. Available online: <https://www.britannica.com/event/Libya-flooding-of-2023> (accessed on 24 March 2024).
9. De La Fuente, A.; Meruane, V.; Meruane, C. Hydrological Early Warning System Based on a Deep Learning Runoff Model Coupled with a Meteorological Forecast. *Water* **2019**, *11*, 1808. [CrossRef]
10. Artinyan, E.; Vincendon, B.; Kroumova, K.; Nedkov, N.; Tsarev, P.; Balabanova, S.; Koshinchanov, G. Flood Forecasting and Alert System for Arda River Basin. *J. Hydrol.* **2016**, *541*, 457–470. [CrossRef]
11. Li, Z. Deep Learning-Based Hydrological Time Series Prediction Model and Interpretability Quantitative Analysis Study. Ph.D. Thesis, Huazhong University of Science and Technology, Wuhan, China, 2023.
12. Li, Z.; Kang, L.; Zhou, L.; Zhu, M. Deep Learning Framework with Time Series Analysis Methods for Runoff Prediction. *Water* **2021**, *13*, 575. [CrossRef]
13. Shen, C. A Transdisciplinary Review of Deep Learning Research and Its Relevance for Water Resources Scientists. *Water Resour. Res.* **2018**, *54*, 8558–8593. [CrossRef]
14. Silver, D.; Huang, A.; Maddison, C.J.; Guez, A.; Sifre, L.; Van Den Driessche, G.; Schrittwieser, J.; Antonoglou, I.; Panneershelvam, V.; Lanctot, M.; et al. Mastering the Game of Go with Deep Neural Networks and Tree Search. *Nature* **2016**, *529*, 484–489. [CrossRef]
15. Jumper, J.; Evans, R.; Pritzel, A.; Green, T.; Figurnov, M.; Ronneberger, O.; Tunyasuvunakool, K.; Bates, R.; Židek, A.; Potapenko, A.; et al. Highly Accurate Protein Structure Prediction with AlphaFold. *Nature* **2021**, *596*, 583–589. [CrossRef] [PubMed]
16. Bello, I.T.; Taiwo, R.; Esan, O.C.; Adegoke, A.H.; Ijaola, A.O.; Li, Z.; Zhao, S.; Wang, C.; Shao, Z.; Ni, M. AI-Enabled Materials Discovery for Advanced Ceramic Electrochemical Cells. *Energy AI* **2024**, *15*, 100317. [CrossRef]
17. Choi, J.B.; Nguyen, P.C.H.; Sen, O.; Udaykumar, H.S.; Baek, S. Artificial Intelligence Approaches for Energetic Materials by Design: State of the Art, Challenges, and Future Directions. *Propellants Explos. Pyrotech.* **2023**, *48*, e202200276. [CrossRef]
18. He, W.; Liu, T.; Ming, W.; Li, Z.; Du, J.; Li, X.; Guo, X.; Sun, P. Progress in Prediction of Remaining Useful Life of Hydrogen Fuel Cells Based on Deep Learning. *Renew. Sustain. Energy Rev.* **2024**, *192*, 114193. [CrossRef]
19. Ming, W.; Sun, P.; Zhang, Z.; Qiu, W.; Du, J.; Li, X.; Zhang, Y.; Zhang, G.; Liu, K.; Wang, Y.; et al. A Systematic Review of Machine Learning Methods Applied to Fuel Cells in Performance Evaluation, Durability Prediction, and Application Monitoring. *Int. J. Hydrog. Energy* **2023**, *48*, 5197–5228. [CrossRef]
20. He, W.; Li, Z.; Liu, T.; Liu, Z.; Guo, X.; Du, J.; Li, X.; Sun, P.; Ming, W. Research Progress and Application of Deep Learning in Remaining Useful Life, State of Health and Battery Thermal Management of Lithium Batteries. *J. Energy Storage* **2023**, *70*, 107868. [CrossRef]

21. Ming, W.; Guo, X.; Zhang, G.; Liu, Y.; Wang, Y.; Zhang, H.; Liang, H.; Yang, Y. Recent Advances in the Precision Control Strategy of Artificial Pancreas. *Med. Biol. Eng. Comput.* **2024**, *62*, 1615–1638. [[CrossRef](#)] [[PubMed](#)]
22. Druzhkov, P.N.; Kustikova, V.D. A Survey of Deep Learning Methods and Software Tools for Image Classification and Object Detection. *Pattern Recognit. Image Anal.* **2016**, *26*, 9–15. [[CrossRef](#)]
23. He, W.; Liu, T.; Han, Y.; Ming, W.; Du, J.; Liu, Y.; Yang, Y.; Wang, L.; Jiang, Z.; Wang, Y.; et al. A Review: The Detection of Cancer Cells in Histopathology Based on Machine Vision. *Comput. Biol. Med.* **2022**, *146*, 105636. [[CrossRef](#)]
24. Ming, W.; Shen, F.; Zhang, H.; Li, X.; Ma, J.; Du, J.; Lu, Y. Defect Detection of LGP Based on Combined Classifier with Dynamic Weights. *Measurement* **2019**, *143*, 211–225. [[CrossRef](#)]
25. Ming, W.; Cao, C.; Zhang, G.; Zhang, H.; Zhang, F.; Jiang, Z.; Yuan, J. Review: Application of Convolutional Neural Network in Defect Detection of 3C Products. *IEEE Access* **2021**, *9*, 135657–135674. [[CrossRef](#)]
26. Ming, W.; Shen, F.; Li, X.; Zhang, Z.; Du, J.; Chen, Z.; Cao, Y. A Comprehensive Review of Defect Detection in 3C Glass Components. *Measurement* **2020**, *158*, 107722. [[CrossRef](#)]
27. Da Silva, D.G.; Meneses, A.A.D.M. Comparing Long Short-Term Memory (LSTM) and Bidirectional LSTM Deep Neural Networks for Power Consumption Prediction. *Energy Rep.* **2023**, *10*, 3315–3334. [[CrossRef](#)]
28. Lee, S.H.; Lee, T.; Kim, S.; Park, S. Energy Consumption Prediction System Based on Deep Learning with Edge Computing. In Proceedings of the 2019 IEEE 2nd International Conference on Electronics Technology (ICET), Chengdu, China, 10–13 May 2019; pp. 473–477.
29. Shu, Z.R.; Jesson, M. Estimation of Weibull Parameters for Wind Energy Analysis across the UK. *J. Renew. Sustain. Energy* **2021**, *13*, 023303. [[CrossRef](#)]
30. Danandeh Mehr, A.; Rikhtehgar Ghiasi, A.; Yaseen, Z.M.; Sorman, A.U.; Abualigah, L. A Novel Intelligent Deep Learning Predictive Model for Meteorological Drought Forecasting. *J. Ambient. Intell. Hum. Comput.* **2023**, *14*, 10441–10455. [[CrossRef](#)]
31. Pullman, M.; Gurung, I.; Maskey, M.; Ramachandran, R.; Christopher, S.A. Applying Deep Learning to Hail Detection: A Case Study. *IEEE Trans. Geosci. Remote Sens.* **2019**, *57*, 10218–10225. [[CrossRef](#)]
32. Chen, X.; Long, Z. E-Commerce Enterprises Financial Risk Prediction Based on FA-PSO-LSTM Neural Network Deep Learning Model. *Sustainability* **2023**, *15*, 5882. [[CrossRef](#)]
33. Huang, J.; Chai, J.; Cho, S. Deep Learning in Finance and Banking: A Literature Review and Classification. *Front. Bus. Res. China* **2020**, *14*, 13. [[CrossRef](#)]
34. Bentivoglio, R.; Isufi, E.; Jonkman, S.N.; Taormina, R. Deep Learning Methods for Flood Mapping: A Review of Existing Applications and Future Research Directions. *Hydrol. Earth Syst. Sci.* **2022**, *26*, 4345–4378. [[CrossRef](#)]
35. Shen, C.; Laloy, E.; Elshorbagy, A.; Albert, A.; Bales, J.; Chang, F.-J.; Ganguly, S.; Hsu, K.-L.; Kifer, D.; Fang, Z.; et al. HESS Opinions: Incubating Deep-Learning-Powered Hydrologic Science Advances as a Community. *Hydrol. Earth Syst. Sci.* **2018**, *22*, 5639–5656. [[CrossRef](#)]
36. Xia, M.; Li, T.; Xu, L.; Liu, L.; de Silva, C.W. Fault Diagnosis for Rotating Machinery Using Multiple Sensors and Convolutional Neural Networks. *IEEE/ASME Trans. Mechatron.* **2018**, *23*, 101–110. [[CrossRef](#)]
37. Geng, Z.; Zhang, Y.; Li, C.; Han, Y.; Cui, Y.; Yu, B. Energy Optimization and Prediction Modeling of Petrochemical Industries: An Improved Convolutional Neural Network Based on Cross-Feature. *Energy* **2020**, *194*, 116851. [[CrossRef](#)]
38. Wang, J.; Li, X.; Li, J.; Sun, Q.; Wang, H. NGCU: A New RNN Model for Time-Series Data Prediction. *Big Data Res.* **2022**, *27*, 100296. [[CrossRef](#)]
39. Ouyang, P.; Yin, S.; Wei, S. A Fast and Power Efficient Architecture to Parallelize LSTM Based RNN for Cognitive Intelligence Applications. In Proceedings of the 2017 54th ACM/EDAC/IEEE Design Automation Conference (DAC), Austin TX USA, 18–22 June 2017; pp. 1–6.
40. Sepahvand, A.; Golkarian, A.; Billa, L.; Wang, K.; Rezaie, F.; Panahi, S.; Samadianfard, S.; Khosravi, K. Evaluation of Deep Machine Learning-Based Models of Soil Cumulative Infiltration. *Earth Sci. Inf.* **2022**, *15*, 1861–1877. [[CrossRef](#)]
41. Han, H.; Hou, J.; Bai, G.; Li, B.; Wang, T.; Li, X.; Gao, X.; Su, F.; Wang, Z.; Liang, Q.; et al. A Deep Learning Technique-Based Automatic Monitoring Method for Experimental Urban Road Inundation. *J. Hydroinformatics* **2021**, *23*, 764–781. [[CrossRef](#)]
42. Fu, G.; Jin, Y.; Sun, S.; Yuan, Z.; Butler, D. The Role of Deep Learning in Urban Water Management: A Critical Review. *Water Res.* **2022**, *223*, 118973. [[CrossRef](#)] [[PubMed](#)]
43. Windheuser, L.; Karanjit, R.; Pally, R.; Samadi, S.; Hubig, N.C. An End-To-End Flood Stage Prediction System Using Deep Neural Networks. *Earth Space Sci.* **2023**, *10*, e2022EA002385. [[CrossRef](#)]
44. Sharma, S.; Kumari, S. Comparison of Machine Learning Models for Flood Forecasting in the Mahanadi River Basin, India. *J. Water Clim. Change* **2024**, *15*, 1629–1652. [[CrossRef](#)]
45. Li, P.; Zhang, J.; Krebs, P. Prediction of Flow Based on a CNN-LSTM Combined Deep Learning Approach. *Water* **2022**, *14*, 993. [[CrossRef](#)]
46. Aderyani, F.R.; Jamshid Mousavi, S.; Jafari, F. Short-Term Rainfall Forecasting Using Machine Learning-Based Approaches of PSO-SVR, LSTM and CNN. *J. Hydrol.* **2022**, *614*, 128463. [[CrossRef](#)]
47. Jiang, L.; Hu, Y.; Xia, X.; Liang, Q.; Soltoggio, A.; Kabir, S.R. A Multi-Scale Map Approach Based on a Deep Learning CNN Model for Reconstructing High-Resolution Urban DEMs. *Water* **2020**, *12*, 1369. [[CrossRef](#)]
48. Haidar, A.; Verma, B. Monthly Rainfall Forecasting Using One-Dimensional Deep Convolutional Neural Network. *IEEE Access* **2018**, *6*, 69053–69063. [[CrossRef](#)]

49. Coulibaly, P.; Baldwin, C.K. Nonstationary Hydrological Time Series Forecasting Using Nonlinear Dynamic Methods. *J. Hydrol.* **2005**, *307*, 164–174. [[CrossRef](#)]
50. Haykin, S.; Li, L. Nonlinear Adaptive Prediction of Nonstationary Signals. *IEEE Trans. Signal Process.* **1995**, *43*, 526–535. [[CrossRef](#)]
51. Güldal, V.; Tongal, H. Comparison of Recurrent Neural Network, Adaptive Neuro-Fuzzy Inference System and Stochastic Models in Eğirdir Lake Level Forecasting. *Water Resour. Manag.* **2010**, *24*, 105–128. [[CrossRef](#)]
52. Cai, B.; Yu, Y. Flood Forecasting in Urban Reservoir Using Hybrid Recurrent Neural Network. *Urban. Clim.* **2022**, *42*, 101086. [[CrossRef](#)]
53. Kim, B.-J.; Lee, Y.-T.; Kim, B.-H. A Study on the Optimal Deep Learning Model for Dam Inflow Prediction. *Water* **2022**, *14*, 2766. [[CrossRef](#)]
54. Wang, Y.; Wang, W.; Zang, H.; Xu, D. Is the LSTM Model Better than RNN for Flood Forecasting Tasks? A Case Study of HuaYuankou Station and LouDe Station in the Lower Yellow River Basin. *Water* **2023**, *15*, 3928. [[CrossRef](#)]
55. Karbasi, M.; Jamei, M.; Ali, M.; Malik, A.; Chu, X.; Farooque, A.A.; Yaseen, Z.M. Development of an Enhanced Bidirectional Recurrent Neural Network Combined with Time-Varying Filter-Based Empirical Mode Decomposition to Forecast Weekly Reference Evapotranspiration. *Agric. Water Manag.* **2023**, *290*, 108604. [[CrossRef](#)]
56. Ayele, E.G.; Ergete, E.T.; Geremew, G.B. Predicting the Peak Flow and Assessing the Hydrologic Hazard of the Kesse Dam, Ethiopia Using Machine Learning and Risk Management Centre-Reservoir Frequency Analysis Software. *J. Water Clim. Change* **2024**, *15*, 370–391. [[CrossRef](#)]
57. Wang, Q.; Huang, J.; Liu, R.; Men, C.; Guo, L.; Miao, Y.; Jiao, L.; Wang, Y.; Shoaib, M.; Xia, X. Sequence-Based Statistical Downscaling and Its Application to Hydrologic Simulations Based on Machine Learning and Big Data. *J. Hydrol.* **2020**, *586*, 124875. [[CrossRef](#)]
58. Kao, I.-F.; Liou, J.-Y.; Lee, M.-H.; Chang, F.-J. Fusing Stacked Autoencoder and Long Short-Term Memory for Regional Multistep-Ahead Flood Inundation Forecasts. *J. Hydrol.* **2021**, *598*, 126371. [[CrossRef](#)]
59. Huang, P.-C. An Effective Alternative for Predicting Coastal Floodplain Inundation by Considering Rainfall, Storm Surge, and Downstream Topographic Characteristics. *J. Hydrol.* **2022**, *607*, 127544. [[CrossRef](#)]
60. Botunac, I.; Bosna, J.; Matetić, M. Optimization of Traditional Stock Market Strategies Using the LSTM Hybrid Approach. *Information* **2024**, *15*, 136. [[CrossRef](#)]
61. Choi, J.Y.; Lee, B. Combining LSTM Network Ensemble via Adaptive Weighting for Improved Time Series Forecasting. *Math. Probl. Eng.* **2018**, *2018*, 2470171. [[CrossRef](#)]
62. Hinch, A.Z.; Tkouat, M. Rolling Element Bearing Remaining Useful Life Estimation Based on a Convolutional Long-Short-Term Memory Network. *Procedia Comput. Sci.* **2018**, *127*, 123–132. [[CrossRef](#)]
63. Jiang, S.; Zheng, Y.; Wang, C.; Babovic, V. Uncovering Flooding Mechanisms Across the Contiguous United States Through Interpretive Deep Learning on Representative Catchments. *Water Resour. Res.* **2022**, *58*, e2021WR030185. [[CrossRef](#)]
64. Hu, C.; Wu, Q.; Li, H.; Jian, S.; Li, N.; Lou, Z. Deep Learning with a Long Short-Term Memory Networks Approach for Rainfall-Runoff Simulation. *Water* **2018**, *10*, 1543. [[CrossRef](#)]
65. Fang, K.; Shen, C.; Kifer, D.; Yang, X. Prolongation of SMAP to Spatiotemporally Seamless Coverage of Continental U.S. Using a Deep Learning Neural Network. *Geophys. Res. Lett.* **2017**, *44*, 11030–11039. [[CrossRef](#)]
66. Le, X.-H.; Ho, H.V.; Lee, G.; Jung, S. Application of Long Short-Term Memory (LSTM) Neural Network for Flood Forecasting. *Water* **2019**, *11*, 1387. [[CrossRef](#)]
67. Frame, J.M.; Kratzert, F.; Klotz, D.; Gauch, M.; Shalev, G.; Gilon, O.; Qualls, L.M.; Gupta, H.V.; Nearing, G.S. Deep Learning Rainfall-Runoff Predictions of Extreme Events. *Hydrol. Earth Syst. Sci.* **2022**, *26*, 3377–3392. [[CrossRef](#)]
68. Kang, J.; Wang, H.; Yuan, F.; Wang, Z.; Huang, J.; Qiu, T. Prediction of Precipitation Based on Recurrent Neural Networks in Jingdezhen, Jiangxi Province, China. *Atmosphere* **2020**, *11*, 246. [[CrossRef](#)]
69. Fang, K.; Shen, C. Near-Real-Time Forecast of Satellite-Based Soil Moisture Using Long Short-Term Memory with an Adaptive Data Integration Kernel. *J. Hydrometeorol.* **2020**, *21*, 399–413. [[CrossRef](#)]
70. Gu, H.; Xu, Y.-P.; Ma, D.; Xie, J.; Liu, L.; Bai, Z. A Surrogate Model for the Variable Infiltration Capacity Model Using Deep Learning Artificial Neural Network. *J. Hydrol.* **2020**, *588*, 125019. [[CrossRef](#)]
71. Arsenault, R.; Martel, J.-L.; Brunet, F.; Brisette, F.; Mai, J. Continuous Streamflow Prediction in Ungauged Basins: Long Short-Term Memory Neural Networks Clearly Outperform Traditional Hydrological Models. *Hydrol. Earth Syst. Sci.* **2023**, *27*, 139–157. [[CrossRef](#)]
72. Lu, D.; Konapala, G.; Painter, S.L.; Kao, S.-C.; Gangrade, S. Streamflow Simulation in Data-Scarce Basins Using Bayesian and Physics-Informed Machine Learning Models. *J. Hydrometeorol.* **2021**, *22*, 1421–1438. [[CrossRef](#)]
73. Koutsovili, E.-I.; Tzoraki, O.; Theodossiou, N.; Tsekouras, G.E. Early Flood Monitoring and Forecasting System Using a Hybrid Machine Learning-Based Approach. *ISPRS Int. J. Geo-Inf.* **2023**, *12*, 464. [[CrossRef](#)]
74. Zou, Y.; Wang, J.; Lei, P.; Li, Y. A Novel Multi-Step Ahead Forecasting Model for Flood Based on Time Residual LSTM. *J. Hydrol.* **2023**, *620*, 129521. [[CrossRef](#)]
75. Xu, Y.; Hu, C.; Wu, Q.; Jian, S.; Li, Z.; Chen, Y.; Zhang, G.; Zhang, Z.; Wang, S. Research on Particle Swarm Optimization in LSTM Neural Networks for Rainfall-Runoff Simulation. *J. Hydrol.* **2022**, *608*, 127553. [[CrossRef](#)]
76. Forghanparast, F.; Mohammadi, G. Using Deep Learning Algorithms for Intermittent Streamflow Prediction in the Headwaters of the Colorado River, Texas. *Water* **2022**, *14*, 2972. [[CrossRef](#)]

77. Dai, Z.; Zhang, M.; Nedjah, N.; Xu, D.; Ye, F. A Hydrological Data Prediction Model Based on LSTM with Attention Mechanism. *Water* **2023**, *15*, 670. [[CrossRef](#)]
78. Xiang, Z.; Yan, J.; Demir, I. A Rainfall-Runoff Model With LSTM-Based Sequence-to-Sequence Learning. *Water Resour. Res.* **2020**, *56*, e2019WR025326. [[CrossRef](#)]
79. Zhang, Y.; Gu, Z.; Thé, J.V.G.; Yang, S.X.; Gharabaghi, B. The Discharge Forecasting of Multiple Monitoring Station for Humber River by Hybrid LSTM Models. *Water* **2022**, *14*, 1794. [[CrossRef](#)]
80. Hu, R.; Fang, F.; Pain, C.C.; Navon, I.M. Rapid Spatio-Temporal Flood Prediction and Uncertainty Quantification Using a Deep Learning Method. *J. Hydrol.* **2019**, *575*, 911–920. [[CrossRef](#)]
81. Xu, L.; Zhang, X.; Yu, H.; Chen, Z.; Du, W.; Chen, N. Incorporating Spatial Autocorrelation into Deformable ConvLSTM for Hourly Precipitation Forecasting. *Comput. Geosci.* **2024**, *184*, 105536. [[CrossRef](#)]
82. Cui, Z.; Zhou, Y.; Guo, S.; Wang, J.; Xu, C.-Y. Effective Improvement of Multi-Step-Ahead Flood Forecasting Accuracy through Encoder-Decoder with an Exogenous Input Structure. *J. Hydrol.* **2022**, *609*, 127764. [[CrossRef](#)]
83. Kao, I.-F.; Zhou, Y.; Chang, L.-C.; Chang, F.-J. Exploring a Long Short-Term Memory Based Encoder-Decoder Framework for Multi-Step-Ahead Flood Forecasting. *J. Hydrol.* **2020**, *583*, 124631. [[CrossRef](#)]
84. Han, Y.; Sun, K.; Yan, J.; Dong, C. Surface Temperature Prediction of East China Sea Based on Variational Mode Decomposition-Long-Short Term Memory-Broad Learning System Hybrid Model. *Laser Optoelectron. Prog.* **2023**, *60*, 0701001. [[CrossRef](#)]
85. Yang, Y.; Dong, J.; Sun, X.; Lima, E.; Mu, Q.; Wang, X. A CFCC-LSTM Model for Sea Surface Temperature Prediction. *IEEE Geosci. Remote Sens. Lett.* **2018**, *15*, 207–211. [[CrossRef](#)]
86. Gauch, M.; Kratzert, F.; Klotz, D.; Nearing, G.; Lin, J.; Hochreiter, S. Rainfall-Runoff Prediction at Multiple Timescales with a Single Long Short-Term Memory Network. *Hydrol. Earth Syst. Sci.* **2021**, *25*, 2045–2062. [[CrossRef](#)]
87. Zhang, K.; Geng, X.; Yan, X.-H. Prediction of 3-D Ocean Temperature by Multilayer Convolutional LSTM. *IEEE Geosci. Remote Sens. Lett.* **2020**, *17*, 1303–1307. [[CrossRef](#)]
88. Sharma, R.K.; Kumar, S.; Padmalal, D.; Roy, A. Streamflow Prediction Using Machine Learning Models in Selected Rivers of Southern India. *Int. J. River Basin Manag.* **2023**, 1–27. [[CrossRef](#)]
89. Kratzert, F.; Klotz, D.; Brenner, C.; Schulz, K.; Herrnegger, M. Rainfall-Runoff Modelling Using Long Short-Term Memory (LSTM) Networks. *Hydrol. Earth Syst. Sci.* **2018**, *22*, 6005–6022. [[CrossRef](#)]
90. Zhao, C.; Liu, C.; Li, W.; Tang, Y.; Yang, F.; Xu, Y.; Quan, L.; Hu, C. Simulation of Urban Flood Process Based on a Hybrid LSTM-SWMM Model. *Water Resour. Manag.* **2023**, *37*, 5171–5187. [[CrossRef](#)]
91. Lees, T.; Buechel, M.; Anderson, B.; Slater, L.; Reece, S.; Coxon, G.; Dadson, S.J. Benchmarking Data-Driven Rainfall-Runoff Models in Great Britain: A Comparison of Long Short-Term Memory (LSTM)-Based Models with Four Lumped Conceptual Models. *Hydrol. Earth Syst. Sci.* **2021**, *25*, 5517–5534. [[CrossRef](#)]
92. Vuong, P.H.; Phu, L.H.; Van Nguyen, T.H.; Duy, L.N.; Bao, P.T.; Trinh, T.D. A Bibliometric Literature Review of Stock Price Forecasting: From Statistical Model to Deep Learning Approach. *Sci. Prog.* **2024**, *107*, 00368504241236557. [[CrossRef](#)]
93. Wang, S.; Chen, J.; Wang, H.; Zhang, D. Degradation Evaluation of Slewing Bearing Using HMM and Improved GRU. *Measurement* **2019**, *146*, 385–395. [[CrossRef](#)]
94. Pan, Z.; Yu, W.; Yi, X.; Khan, A.; Yuan, F.; Zheng, Y. Recent Progress on Generative Adversarial Networks (GANs): A Survey. *IEEE Access* **2019**, *7*, 36322–36333. [[CrossRef](#)]
95. Alipour-Fard, T.; Arefi, H. Structure Aware Generative Adversarial Networks for Hyperspectral Image Classification. *IEEE J. Sel. Top. Appl. Earth Obs. Remote Sens.* **2020**, *13*, 5424–5438. [[CrossRef](#)]
96. Xie, H.; Randall, M.; Chau, K. Green Roof Hydrological Modelling With GRU and LSTM Networks. *Water Resour. Manag.* **2022**, *36*, 1107–1122. [[CrossRef](#)]
97. Sadeghi Tabas, S.; Samadi, S. Variational Bayesian Dropout with a Gaussian Prior for Recurrent Neural Networks Application in Rainfall-Runoff Modeling. *Environ. Res. Lett.* **2022**, *17*, 065012. [[CrossRef](#)]
98. Cho, M.; Kim, C.; Jung, K.; Jung, H. Water Level Prediction Model Applying a Long Short-Term Memory (LSTM)-Gated Recurrent Unit (GRU) Method for Flood Prediction. *Water* **2022**, *14*, 2221. [[CrossRef](#)]
99. Zhang, Y.; Zhou, Z.; Van Griensven Thé, J.; Yang, S.X.; Gharabaghi, B. Flood Forecasting Using Hybrid LSTM and GRU Models with Lag Time Preprocessing. *Water* **2023**, *15*, 3982. [[CrossRef](#)]
100. Kilinc, H.C.; Yurtsever, A. Short-Term Streamflow Forecasting Using Hybrid Deep Learning Model Based on Grey Wolf Algorithm for Hydrological Time Series. *Sustainability* **2022**, *14*, 3352. [[CrossRef](#)]
101. Chhetri, M.; Kumar, S.; Pratim Roy, P.; Kim, B.-G. Deep BLSTM-GRU Model for Monthly Rainfall Prediction: A Case Study of Simtokha, Bhutan. *Remote Sens.* **2020**, *12*, 3174. [[CrossRef](#)]
102. Guo, W.-D.; Chen, W.-B.; Chang, C.-H. Prediction of Hourly Inflow for Reservoirs at Mountain Catchments Using Residual Error Data and Multiple-Ahead Correction Technique. *Hydrol. Res.* **2023**, *54*, 1072–1093. [[CrossRef](#)]
103. Zhao, R.; Wang, D.; Yan, R.; Mao, K.; Shen, F.; Wang, J. Machine Health Monitoring Using Local Feature-Based Gated Recurrent Unit Networks. *IEEE Trans. Ind. Electron.* **2018**, *65*, 1539–1548. [[CrossRef](#)]
104. Gu, B.; Shen, H.; Lei, X.; Hu, H.; Liu, X. Forecasting and Uncertainty Analysis of Day-Ahead Photovoltaic Power Using a Novel Forecasting Method. *Appl. Energy* **2021**, *299*, 117291. [[CrossRef](#)]
105. Onan, A. Bidirectional Convolutional Recurrent Neural Network Architecture with Group-Wise Enhancement Mechanism for Text Sentiment Classification. *J. King Saud. Univ. Comput. Inf. Sci.* **2022**, *34*, 2098–2117. [[CrossRef](#)]

106. Stateczny, A.; Narahari, S.C.; Vurubindi, P.; Guptha, N.S.; Srinivas, K. Underground Water Level Prediction in Remote Sensing Images Using Improved Hydro Index Value with Ensemble Classifier. *Remote Sens.* **2023**, *15*, 2015. [[CrossRef](#)]
107. Li, X.; Song, G.; Du, Z. Hybrid Model of Generative Adversarial Network and Takagi-Sugeno for Multidimensional Incomplete Hydrological Big Data Prediction. *Concurr. Comput. Pract. Exp.* **2021**, *33*, e5713. [[CrossRef](#)]
108. Hofmann, J.; Schüttrumpf, H. floodGAN: Using Deep Adversarial Learning to Predict Pluvial Flooding in Real Time. *Water* **2021**, *13*, 2255. [[CrossRef](#)]
109. do Lago, C.A.F.; Giacomoni, M.H.; Bentivoglio, R.; Taormina, R.; Gomes, M.N.; Mendiondo, E.M. Generalizing Rapid Flood Predictions to Unseen Urban Catchments with Conditional Generative Adversarial Networks. *J. Hydrol.* **2023**, *618*, 129276. [[CrossRef](#)]
110. Laloy, E.; Héroult, R.; Jacques, D.; Linde, N. Training-Image Based Geostatistical Inversion Using a Spatial Generative Adversarial Neural Network. *Water Resour. Res.* **2018**, *54*, 381–406. [[CrossRef](#)]
111. Tripathy, K.P.; Mishra, A.K. Deep Learning in Hydrology and Water Resources Disciplines: Concepts, Methods, Applications, and Research Directions. *J. Hydrol.* **2024**, *628*, 130458. [[CrossRef](#)]
112. Ren, J.; Ren, B.; Zhang, Q.; Zheng, X. A Novel Hybrid Extreme Learning Machine Approach Improved by K Nearest Neighbor Method and Fireworks Algorithm for Flood Forecasting in Medium and Small Watershed of Loess Region. *Water* **2019**, *11*, 1848. [[CrossRef](#)]
113. Zhang, E. Investigating Front Variations of Greenland Glaciers Using Multi-Temporal Remote Sensing Images and Deep Learning. Ph.D. Thesis, Hong Kong University of Science and Technology (Hong Kong), Hong Kong, China, 2020.
114. Zhou, Y.; Wu, Z.; Jiang, M.; Xu, H.; Yan, D.; Wang, H.; He, C.; Zhang, X. Real-Time Prediction and Ponding Process Early Warning Method at Urban Flood Points Based on Different Deep Learning Methods. *J. Flood Risk Manag.* **2024**, *17*, e12964. [[CrossRef](#)]
115. Bui, Q.-T.; Nguyen, Q.-H.; Nguyen, X.L.; Pham, V.D.; Nguyen, H.D.; Pham, V.-M. Verification of Novel Integrations of Swarm Intelligence Algorithms into Deep Learning Neural Network for Flood Susceptibility Mapping. *J. Hydrol.* **2020**, *581*, 124379. [[CrossRef](#)]
116. Chew, A.W.Z.; He, R.; Zhang, L. Multiscale Homogenized Predictive Modelling of Flooding Surface in Urban Cities Using Physics-Induced Deep AI with UPC. *J. Clean. Prod.* **2022**, *363*, 132455. [[CrossRef](#)]
117. Zhao, Q.; Zhu, Y.; Shu, K.; Wan, D.; Yu, Y.; Zhou, X.; Liu, H. Joint Spatial and Temporal Modeling for Hydrological Prediction. *IEEE Access* **2020**, *8*, 78492–78503. [[CrossRef](#)]
118. Wang, W.; Yan, H.; Lu, X.; He, Y.; Liu, T.; Li, W.; Li, P.; Xu, F. Drainage Pattern Recognition Method Considering Local Basin Shape Based on Graph Neural Network. *Int. J. Digit. Earth* **2023**, *16*, 593–619. [[CrossRef](#)]
119. Alom, M.Z.; Taha, T.M.; Yakopcic, C.; Westberg, S.; Sidike, P.; Nasrin, M.S.; Hasan, M.; Van Essen, B.C.; Awwal, A.A.S.; Asari, V.K. A State-of-the-Art Survey on Deep Learning Theory and Architectures. *Electronics* **2019**, *8*, 292. [[CrossRef](#)]
120. Kumari, P.; Toshniwal, D. Deep Learning Models for Solar Irradiance Forecasting: A Comprehensive Review. *J. Clean. Prod.* **2021**, *318*, 128566. [[CrossRef](#)]
121. Van Houdt, G.; Mosquera, C.; Nápoles, G. A Review on the Long Short-Term Memory Model. *Artif. Intell. Rev.* **2020**, *53*, 5929–5955. [[CrossRef](#)]
122. Hoang, M.T.; Yuen, B.; Dong, X.; Lu, T.; Westendorp, R.; Reddy, K. Recurrent Neural Networks for Accurate RSSI Indoor Localization. *IEEE Internet Things J.* **2019**, *6*, 10639–10651. [[CrossRef](#)]
123. Chen, C.; Jiang, J.; Zhou, Y.; Lv, N.; Liang, X.; Wan, S. An Edge Intelligence Empowered Flooding Process Prediction Using Internet of Things in Smart City. *J. Parallel Distrib. Comput.* **2022**, *165*, 66–78. [[CrossRef](#)]
124. Zulqarnain, M.; Ghazali, R.; Aamir, M.; Hassim, Y.M.M. An Efficient Two-State GRU Based on Feature Attention Mechanism for Sentiment Analysis. *Multimed. Tools Appl.* **2024**, *83*, 3085–3110. [[CrossRef](#)]
125. Liu, Y.; Pei, A.; Wang, F.; Yang, Y.; Zhang, X.; Wang, H.; Dai, H.; Qi, L.; Ma, R. An Attention-Based Category-Aware GRU Model for the next POI Recommendation. *Int. J. Intell. Syst.* **2021**, *36*, 3174–3189. [[CrossRef](#)]
126. Ming, W.; Guo, X.; Xu, Y.; Zhang, G.; Jiang, Z.; Li, Y.; Li, X. Progress in Non-Traditional Machining of Amorphous Alloys. *Ceram. Int.* **2023**, *49*, 1585–1604. [[CrossRef](#)]
127. Ming, W.; Zhang, Z.; Wang, S.; Zhang, Y.; Shen, F.; Zhang, G. Comparative Study of Energy Efficiency and Environmental Impact in Magnetic Field Assisted and Conventional Electrical Discharge Machining. *J. Clean. Prod.* **2019**, *214*, 12–28. [[CrossRef](#)]
128. Ming, W.; Guo, X.; Zhang, G.; Hu, S.; Liu, Z.; Xie, Z.; Zhang, S.; Duan, L. Optimization of Process Parameters and Performance for Machining Inconel 718 in Renewable Dielectrics. *Alex. Eng. J.* **2023**, *79*, 164–179. [[CrossRef](#)]
129. Chen, X.; Wu, Y.; He, X.; Ming, W. A Comprehensive Review of Deep Learning-Based PCB Defect Detection. *IEEE Access* **2023**, *11*, 139017–139038. [[CrossRef](#)]
130. Zhao, X.; Zhao, Y.; Hu, S.; Wang, H.; Zhang, Y.; Ming, W. Progress in Active Infrared Imaging for Defect Detection in the Renewable and Electronic Industries. *Sensors* **2023**, *23*, 8780. [[CrossRef](#)] [[PubMed](#)]
131. Zhang, Z.; Ming, W.; Zhang, Y.; Yin, L.; Xue, T.; Yu, H.; Chen, Z.; Liao, D.; Zhang, G. Analyzing Sustainable Performance on High-Precision Molding Process of 3D Ultra-Thin Glass for Smart Phone. *J. Clean. Prod.* **2020**, *255*, 120196. [[CrossRef](#)]
132. Wang, J.; Zhang, C. Software Reliability Prediction Using a Deep Learning Model Based on the RNN Encoder–Decoder. *Reliab. Eng. Syst. Saf.* **2018**, *170*, 73–82. [[CrossRef](#)]
133. Forootan, M.M.; Larki, I.; Zahedi, R.; Ahmadi, A. Machine Learning and Deep Learning in Energy Systems: A Review. *Sustainability* **2022**, *14*, 4832. [[CrossRef](#)]

134. Jin, L.W.; Zhong, Z.Y.; Yang, Z.; Yang, W.X.; Sun, J. Applications of Deep Learning for Handwritten Chinese Character Recognition: A Review. *Acta Autom. Sin.* **2016**, *42*, 1125–1141. [[CrossRef](#)]
135. Jiang, F.; Fu, Y.; Gupta, B.B.; Liang, Y.; Rho, S.; Lou, F.; Meng, F.; Tian, Z. Deep Learning Based Multi-Channel Intelligent Attack Detection for Data Security. *IEEE Trans. Sustain. Comput.* **2020**, *5*, 204–212. [[CrossRef](#)]
136. Lu, N.; Wu, Y.; Feng, L.; Song, J. Deep Learning for Fall Detection: Three-Dimensional CNN Combined With LSTM on Video Kinematic Data. *IEEE J. Biomed. Health Inform.* **2019**, *23*, 314–323. [[CrossRef](#)]
137. Wang, X.; Wang, X.; Yu, M.; Li, C.; Song, D.; Ren, P.; Wu, J. MesoGRU: Deep Learning Framework for Mesoscale Eddy Trajectory Prediction. *IEEE Geosci. Remote Sens. Lett.* **2022**, *19*, 1–5. [[CrossRef](#)]
138. Yang, Y.-F.; Liao, S.-M.; Liu, M.-B. Dynamic Prediction of Moving Trajectory in Pipe Jacking: GRU-Based Deep Learning Framework. *Front. Struct. Civ. Eng.* **2023**, *17*, 994–1010. [[CrossRef](#)]
139. Konapala, G.; Kao, S.-C.; Painter, S.L.; Lu, D. Machine Learning Assisted Hybrid Models Can Improve Streamflow Simulation in Diverse Catchments across the Conterminous US. *Environ. Res. Lett.* **2020**, *15*, 104022. [[CrossRef](#)]
140. Wang, Y.-H. Bridging the Gap Between the Physical-Conceptual Approach and Machine Learning for Modeling Hydrological Systems. Doctoral Dissertation, The University of Arizona, Tucson, AZ, USA, 2023.
141. Townshend, R.J.L.; Eismann, S.; Watkins, A.M.; Rangan, R.; Karelina, M.; Das, R.; Dror, R.O. Geometric Deep Learning of RNA Structure. *Science* **2021**, *373*, 1047–1051. [[CrossRef](#)]
142. Raissi, M.; Yazdani, A.; Karniadakis, G.E. Hidden Fluid Mechanics: Learning Velocity and Pressure Fields from Flow Visualizations. *Science* **2020**, *367*, 1026–1030. [[CrossRef](#)]
143. Fang, T.; Chen, Y.; Tan, H.; Cao, J.; Liao, J.; Huang, L. Flood Risk Evaluation in the Middle Reaches of the Yangtze River Based on Eigenvector Spatial Filtering Poisson Regression. *Water* **2019**, *11*, 1969. [[CrossRef](#)]
144. Darand, M.; Dostkamyani, M.; Rehmani, M.I.A. Spatial Autocorrelation Analysis of Extreme Precipitation in Iran. *Russ. Meteorol. Hydrol.* **2017**, *42*, 415–424. [[CrossRef](#)]
145. Zhuang, Q.; Liu, S.; Zhou, Z. Spatial Heterogeneity Analysis of Short-Duration Extreme Rainfall Events in Megacities in China. *Water* **2020**, *12*, 3364. [[CrossRef](#)]
146. Kumar, R.; Livneh, B.; Samaniego, L. Toward Computationally Efficient Large-Scale Hydrologic Predictions with a Multiscale Regionalization Scheme. *Water Resour. Res.* **2013**, *49*, 5700–5714. [[CrossRef](#)]

Disclaimer/Publisher’s Note: The statements, opinions and data contained in all publications are solely those of the individual author(s) and contributor(s) and not of MDPI and/or the editor(s). MDPI and/or the editor(s) disclaim responsibility for any injury to people or property resulting from any ideas, methods, instructions or products referred to in the content.